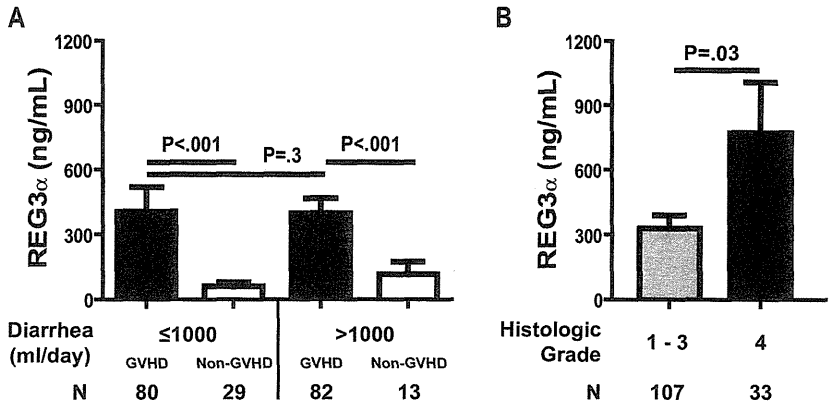

Figure 3. REG3α expression according to severity of GVHD at diagnosis. Patients were classified by volume of diarrhea (A) and histologic grade (B).

Causes of 1-year mortality for these patients are listed in supplemental Table 9.

Of the 162 patients with diarrhea at the onset of GVHD, we possessed all 4 data points of clinical stage, histologic grade, REG3α concentration, and serum albumin level in 140 patients. As shown in Table 3, the plasma concentration of REG3α, the clinical severity of GVHD, the histologic severity, and serum albumin level at GVHD diagnosis independently predicted lack of response to GVHD therapy 4 weeks following treatment after adjustment for the aforementioned risk factors (odds ratios: 4.8, 3.9, 18.9, and 2.5, respectively). When lack of response to therapy and NRM were modeled simultaneously on all 4 parameters, all but albumin remained statistically significant. When only advanced clinical stage and severe histologic grade were considered, NRM was 71% (Figure 4E). The inclusion of high REG3α concentration further risk-stratified patients who had either advanced clinical

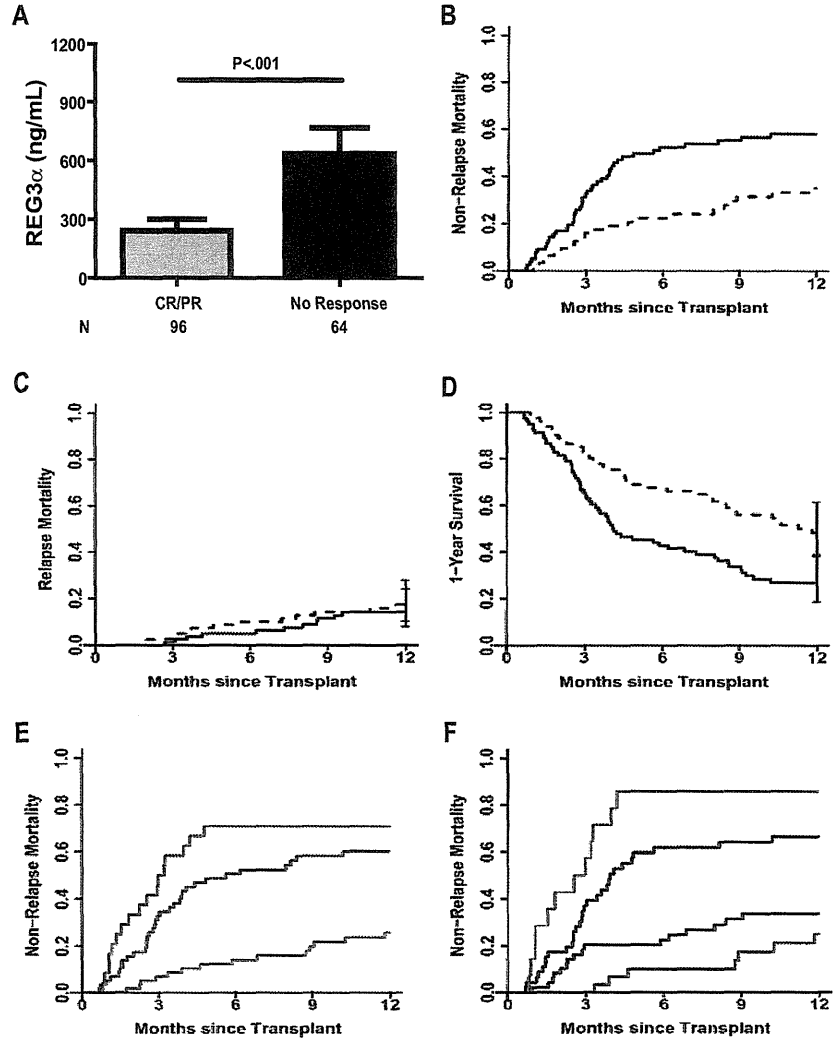

Figure 4. Prognostic value of REG3α concentrations at onset of GVHD. (A) Patients were classified by response to GVHD therapy after 4 weeks (N = 160). (B-D) Patients were classified by REG3α concentration: low (≤ 151 ng/mL, n = 81; thin line) and high (> 151 ng/mL, n = 81; thick line). (B) NRM (34% vs 59%, $P < .001$) (C) Relapse mortality (17% vs 14%, $P = .59$). (D) One-year survival (48% vs 27%, $P = .001$). All P values are adjusted for donor source, HLA match, conditioning intensity, recipient age, and baseline disease severity according to the Center for International Blood and Marrow Transplant Research (CIBMTR) guidelines. (E) One-year NRM for patients classified by number of risk factors at GVHD onset, using clinical stage (high risk = stage 2-4) and histologic grade (high risk = grade 4); 0 (purple, NRM = 26%); 1 (red, NRM = 60%); 2 (blue, NRM = 71%); 0 vs 1, $P < .001$; 1 vs 2, $P = .006$. (F) One-year NRM for patients classified by number of risk factors at the time of GVHD diagnosis as in panel E and including REG3α concentration (high risk > 151 ng/mL); 0 (purple, NRM = 25%); 1 (red, NRM = 34%); 2 (purple, NRM = 66%); 3 (brown, NRM = 86%); 0 vs 1, $P = .2$; 1 vs 2, $P < .001$; 2 vs 3, $P < .001$.

Table 3. REG3α concentrations and characteristics at onset of GVHD diarrhea predict 4-week response to GVHD therapy and 1-year NRM

	Independent		Simultaneous	
	Ratio	P*	Ratio	P*
No response to treatment (at 4 wk)	Odds		Odds	
REG3α (high vs low)	4.8	< .001	5.7	.001
GVHD GI onset stage (2-4 vs 1)	3.9	.001	3.0	.027
Histologic grade (4 vs 1-3)	18.9	< .001	16.7	< .001
Albumin (low vs high)	2.5	.02	1.4	.5
1-y NRM	Hazard		Hazard	
REG3α (high vs low)	2.2	.003	2.4	.002
GVHD GI onset stage (2-4 vs 1)	3.0	< .001	3.1	< .001
Histologic grade (4 vs 1-3)	3.6	< .001	2.9	< .001
Albumin (low vs high)	2.3	.004	1.6	.2

NRM indicates nonrelapse mortality; and GI, gastrointestinal.

*Adjusted for age, donor type, HLA match, conditioning intensity, and disease status at transplantation.

stage or histologic severity (Figure 4F; 34% vs 66% for 1 or 2 risk factors, respectively, $P < .001$), and patients who had all 3 risk factors experienced significantly greater NRM than those with any 2 of the risk factors (86% vs 66%, $P < .001$). Details of patient risk factors are listed in supplemental Table 10; NRM by all other risk factor combinations are shown in supplemental Figure 7.

Discussion

The etiology of diarrhea following HCT presents a common diagnostic dilemma.[30,31] We identified REG3α as a candidate biomarker specific for lower GI GVHD through an unbiased, in-depth tandem MS-based discovery approach that can quantify proteins at low concentrations and that we previously used successfully to identify elafin as a plasma biomarker specific for GVHD of the skin.[17] Our discovery approach identified 74 proteins that were increased at least 2-fold in the plasma from patients with GI GVHD. Of note, the list did not include cytokeratin-18 (KRT18), which has been reported to be specific for both liver and intestinal GVHD.[32] This discrepancy may be explained by limitations in proteomics technology and the significantly later acquisition times of samples in the earlier report.

REG proteins act downstream of IL-22 to protect the epithelial barrier function of the intestinal mucosa[33,34] through the binding of bacterial peptidoglycans.[13] Intestinal stem cells (ISCs) are principal cellular targets of GVHD in the GI tract,[3,35] where intestinal flora are critical for amplification of GVHD damage.[36,37] A leading hypothesis is that ISCs are protected by antibacterial proteins such as REG3α secreted by neighboring Paneth cells into the crypt microenvironment.[38] If death of an ISC eventually manifests itself as denudation of the mucosa, the patchy nature of GVHD histologic damage may be explained as the lack of mucosal regeneration following the dropout of individual ISCs.[3,35] REG3α reduces the inflammation of human intestinal crypts in vitro,[14,39] and its administration protects ISCs and prevents GI epithelial damage in vivo,[34] raising interesting therapeutic possibilities for this molecule.

REG3α plasma concentrations correlate with disease activity in inflammatory bowel disease, and can distinguish infectious and autoimmune causes of diarrhea.[14] The correlation of mucosal denudation (histologic grade 4) with high REG3α concentrations suggests that microscopic breaches in the mucosal epithelial barrier caused by severe GVHD permit REG3α to traverse into the systemic circulation. The tight proximity of Paneth cells with ISCs concentrates their secretory contents in that vicinity, so that mucosal barrier disruption caused by stem cell dropout may preferentially allow Paneth cell secretions, including REG3α, to traverse into the bloodstream. We hypothesize that plasma levels of REG3α may therefore serve as a surrogate marker for the cumulative area of these breaches to GI mucosal barrier integrity, a parameter impossible to measure by individual tissue biopsies. Such an estimate of total damage to the mucosal barrier may also help explain the prognostic value of REG3α with respect to therapy responsiveness and NRM.

In this study, 3 high-risk parameters each independently correlated with lack of response to treatment and to higher NRM: elevated plasma REG3α concentration, higher clinical stage of GVHD at diagnosis and grade 4 histologic severity. All 3 of these values thus provided important prognostic information before the initiation of therapy rather than at the time of maximum grade of GVHD, which by definition includes responsiveness to therapy.[5,6,11] This study confirms earlier reports where higher clinical stage of GI GVHD[5,6] and more severe histology correlated with worse survival.[10] In our study the 1-year NRM was 33% (22 of 67 patients) in patients with clinical stage I lower GI GVHD when considering clinical severity alone. Seven of 8 patients (88%) who had the 2 other high risk factors present experienced 1-year NRM while 25% (15 of 59) of patients with 1 or no risk factors experienced 1-year NRM. In this regard it should be noted that REG3α levels did not obviate the need for biopsy. If the prognostic value of REG3α is confirmed in additional patients, we believe the integration of clinical stage, histologic grade and REG3α plasma concentrations into a single grading system will permit better risk stratification and rapid identification of those patients with severe GI damage in whom standard treatment is likely to be insufficient.

Acknowledgments

The authors thank Dr David Beer for critical reading of the manuscript, the clinicians of the University of Michigan Blood and Marrow Transplantation division: Daniel Couriel, Greg Yanik, Carrie Kitko, James Connelly, Craig Byersdorfer, Shin Mineishi, John Magenau, Ed Peres, and Attaphol Pawarode; David Hanauer for assistance with data abstraction using the EMERSE tool; the University of Michigan clinical research support staff: Joel Whitfield, Dawn Jones, and Connie Varner; the University of Michigan BMT division data managers: Pamela Jones, Rachel Young, Charlotte Zinkus, Katherine Archangeli, Tamara Cummings, Sean Kelley, and Jennifer Lay-Luskin; the members of the Paczesny laboratory: Aurelie Gomez, Megan Conlon, and Jeffrey Crawford; the members of the Hanash laboratory: Hong Wang, Vitor Faca, and Sharon Pitteri; and the Seattle Proteomics Core, particularly Phillip Gafken and Jason Hogan.

This work was supported by National Institutes of Health (NIH) grants RC1-HL-101102, P01-CA039542, T32-HL007622, the Hartwell Foundation, and the Doris Duke Charitable Foundation. Informatics assistance with data abstraction and the EMERSE tool was provided by the University of Michigan Cancer Center's (UMCC) Biomedical Informatics Core with partial support from the NIH through the UMCC Support grant (CA46592). Partial funding for the LTQ-FT mass spectrometer used in this work was generously provided by the M. J. Murdock Charitable Trust.

J.L.M.F. is a clinical research professor of the American Cancer Society and a visiting fellow of the Oxford All Souls College. S.P. is an investigator of the Eric Hartwell fund and the Amy Strelzer Manasevit Research Program.

Authorship

Contribution: J.L.M.F. planned the study, interpreted the data, and wrote the manuscript; A.C.H. designed and planned the experiments, performed research, performed data collection and quality assurance, analyzed data, and wrote the manuscript; J.K.G. and E. Huber performed pathology evaluations and wrote the manuscript; T.M.B. was the study statistician and wrote the manuscript; E. Holler, T.T., J.E.L., S.W.J.C., K. L., K.A., and P.R. contributed to patient accrual, clinical data collection and quality assurance, research discussion, and wrote the manuscript; M.V.L. performed experiments and wrote the manuscript; A.C., Q.Z., and S.H. performed the proteomics experiments, interpreted data, and wrote the manuscript; and S.P. conceived and planned the study design, performed experiments, interpreted data, and wrote the manuscript.

Conflict-of-interest disclosure: The authors declare no competing financial interests.

Correspondence: Dr Sophie Paczesny, Blood and Marrow Transplant Program, University of Michigan Comprehensive Cancer Center, Rm 6410, 1500 E Medical Center Dr, Ann Arbor, MI, 48109-5942; e-mail: sophiep@med.umich.edu.

References

1. Cutler C, Antin JH. Manifestation and treatment of acute graft-versus-host-disease. In: Appelbaum F, Forman SJ, Negrin RS, Blume KG, eds. *Thomas' Hematopoietic Cell Transplantation.* Oxford, United Kingdom: Blackwell Publishing Ltd; 2009: 1287-1303.
2. Welniak LA, Blazar BR, Murphy WJ. Immunobiology of allogeneic hematopoietic stem cell transplantation. *Annu Rev Immunol.* 2007;25:139-170.
3. Mowat A, Socie G. Intestinal graft-vs.-host disease. In: Ferrara JLM, Cooke KR, Deeg HJ, eds. *Graft-vs-Host Disease.* New York, NY: Marcel Dekker; 2004:279-327.
4. Ferrara JL, Levine JE, Reddy P, Holler E. Graft-versus-host disease. *Lancet.* 2009;373(9674): 1550-1561.
5. Martin PJ, McDonald GB, Sanders JE, et al. Increasingly frequent diagnosis of acute gastrointestinal graft-versus-host disease after allogeneic hematopoietic cell transplantation. *Biol Blood Marrow Transpl.* 2004;10(5):320-327.
6. MacMillan ML, Weisdorf DJ, Wagner JE, et al. Response of 443 patients to steroids as primary therapy for acute graft-versus-host disease: comparison of grading systems. *Biol Blood Marrow Transpl.* 2002;8(7):387-394.
7. Przepiorka D, Weisdorf D, Martin P, et al. 1994 Consensus Conference on Acute GVHD Grading. *Bone Marrow Transpl.* 1995;15(6):825-828.
8. Shulman HM, Kleiner D, Lee SJ, et al. Histopathologic diagnosis of chronic graft-versus-host disease: National Institutes of Health Consensus Development Project on Criteria for Clinical Trials in Chronic Graft-versus-Host Disease: II. Pathology Working Group Report. *Biol Blood Marrow Transpl.* 2006;12(1):31-47.
9. Washington K, Jagasia M. Pathology of graft-versus-host disease in the gastrointestinal tract. *Hum Pathol.* 2009;40(7):909-917.
10. Ertault-Daneshpouy M, Leboeuf C, Lemann M, et al. Pericapillary hemorrhage as criterion of severe human digestive graft-versus-host disease. *Blood.* 2004;103(12):4681-4684.
11. Weisdorf D, Haake R, Blazar B, et al. Treatment of moderate/severe acute graft-versus-host disease after allogeneic bone marrow transplantation: an analysis of clinical risk features and outcome. *Blood.* 1990;75(4):1024-1030.
12. Deeg HJ. How I treat refractory acute GVHD. *Blood.* 2007;109(10):4119-4126.
13. Cash HL, Whitham CV, Behrendt CL, Hooper LV. Symbiotic bacteria direct expression of an intestinal bactericidal lectin. *Science.* 2006;313(5790): 1126-1130.
14. Gironella M, Iovanna JL, Sans M, et al. Anti-inflammatory effects of pancreatitis associated protein in inflammatory bowel disease. *Gut.* 2005; 54(9):1244-1253.
15. Faca V, Coram M, Phanstiel D, et al. Quantitative analysis of acrylamide labeled serum proteins by LC-MS/MS. *J Proteome Res.* 2006;5(8):2009-2018.
16. Faca V, Pitteri SJ, Newcomb L, et al. Contribution of protein fractionation to depth of analysis of the serum and plasma proteomes. *J Proteome Res.* 2007;6(9):3558-3565.
17. Paczesny S, Braun T, Levine JE, et al. Elafin is a biomarker of graft-versus-host disease of the skin. *Sci Transl Medicine.* 2010;2(13):50-57.
18. Lemer KG, Kao GF, Storb R, Buckner CD, Clift RA, Thomas ED. Histopathology of graft-vs.-host reaction (GvHR) in human recipients of marrow from HL-A-matched sibling donors. *Transplant Proc.* 1974;6(4):367-371.
19. Paczesny S, Krijanovski OI, Braun TM, et al. A biomarker panel for acute graft-versus-host disease. *Blood.* 2009;113(2):273-278.
20. Fine JP, Gray RJ. A proportional hazards model for the subdistribution of a competing risk. *J Am Stat Assoc.* 1999;94:496-509.
21. Skidgel RA, Erdos EG. Structure and function of human plasma carboxypeptidase N, the anaphylatoxin inactivator. *Int Immunopharmacol.* 2007; 7(14):1888-1899.
22. Marchbank T, Freeman TC, Playford RJ. Human pancreatic secretory trypsin inhibitor. Distribution, actions and possible role in mucosal integrity and repair. *Digestion.* 1998;59(3):167-174.
23. Mykkanen OM, Gronholm M, Ronty M, et al. Characterization of human palladin, a microfilament-associated protein. *Mol Biol Cell.* 2001; 12(10):3060-3073.
24. Watanabe T, Yonekura H, Terazono K, Yamamoto H, Okamoto H. Complete nucleotide sequence of human reg gene and its expression in normal and tumoral tissues. The reg protein, pancreatic stone protein, and pancreatic thread protein are one and the same product of the gene. *J Biol Chem.* 1990;265(13):7432-7439.
25. Christa L, Carnot F, Simon MT, et al. HIP/PAP is an adhesive protein expressed in hepatocarcinoma, normal Paneth, and pancreatic cells. *Am J Physiol.* 1996;271(6 Pt 1):G993-G1002.
26. Ayabe T, Satchell DP, Wilson CL, Parks WC, Selsted ME, Ouellette AJ. Secretion of microbicidal alpha-defensins by intestinal Paneth cells in response to bacteria. *Nat Immunol.* 2000;1(2): 113-118.
27. Weisdorf SA, Salati LM, Longsdorf JA, Ramsay NK, Sharp HL. Graft-versus-host disease of the intestine: a protein losing enteropathy characterized by fecal alpha 1-antitrypsin. *Gastroenterology.* 1983;85(5):1076-1081.
28. MacMillan ML, DeFor TE, Weisdorf DJ. The best endpoint for acute GVHD treatment trials. *Blood.* 2010;115(26):5412-5417.
29. Levine JE, Logan B, Wu J, et al. Graft-versus-host disease treatment: predictors of survival. *Biol Blood Marrow Transplant.* 2010;16(12):1693-1699.
30. Cox GJ, Matsui SM, Lo RS, et al. Etiology and outcome of diarrhea after marrow transplantation: a prospective study. *Gastroenterology.* 1994; 107(5):1398-1407.
31. Barker CC, Anderson RA, Sauve RS, Butzner JD. GI complications in pediatric patients post-BMT. *Bone Marrow Transplant.* 2005;36(1):51-58.
32. Luft T, Conzelmann M, Benner A, et al. Serum cytokeratin-18 fragments as quantitative markers of epithelial apoptosis in liver and intestinal graft-versus-host disease. *Blood.* 2007;110(13):4535-4542.
33. Sanos SL, Vonarbourg C, Mortha A, Diefenbach A. Control of epithelial cell function by interleukin-22-producing RORgammat(+) innate lymphoid cells. *Immunology.* 2011;132(4):453-465.
34. Zheng Y, Valdez PA, Danilenko DM, et al. Interleukin-22 mediates early host defense against attaching and effacing bacterial pathogens. *Nat Med.* 2008;14(3):282-289.
35. Takashima S, Kadowaki M, Aoyama K, et al. The Wnt agonist R-spondin1 regulates systemic graft-versus-host disease by protecting intestinal stem cells. *J Exp Med.* 2011;208(2):285-294.
36. van Bekkum DW, Roodenburg J, Heidt PJ, van der Waaij D. Mitigation of secondary disease of allogeneic mouse radiation chimeras by modification of the intestinal microflora. *J Natl Cancer Inst.* 1974;52(2):401-404.
37. Gerbitz A, Schultz M, Wilke A, et al. Probiotic effects on experimental graft-versus-host disease: let them eat yogurt. *Blood.* 2004;103(11):4365-4367.
38. Elphick DA, Mahida YR. Paneth cells: their role in innate immunity and inflammatory disease. *Gut.* 2005;54(12):1802-1809.
39. Closa D, Motoo Y, Iovanna JL. Pancreatitis-associated protein: from a lectin to an anti-inflammatory cytokine. *World J Gastroenterol.* 2007;13(2):170-174.

Brief report

Plasma biomarkers of lower gastrointestinal and liver acute GVHD

Andrew C. Harris,[1] James L. M. Ferrara,[1] Thomas M. Braun,[2] Ernst Holler,[3] Takanori Teshima,[4] John E. Levine,[1] Sung W. Choi,[1] Karin Landfried,[3] Koichi Akashi,[4] Mark Vander Lugt,[1] Daniel R. Couriel,[1] Pavan Reddy,[1] and Sophie Paczesny[1]

[1]Blood and Marrow Transplant Program and [2]Department of Biostatistics, The University of Michigan, Ann Arbor, MI; [3]Department of Hematology/Oncology, University Medical Center Regensburg, Regensburg, Germany; and [4]Center for Cellular and Molecular Medicine, Kyushu University Graduate School of Science, Fukuoka, Japan

The lower gastrointestinal tract (LGI) and liver are the GVHD target organs most associated with treatment failure and nonrelapse mortality. We recently identified regenerating islet-derived 3-α (REG3α) as a plasma biomarker of LGI GVHD. We compared REG3α with 2 previously reported GI and liver GVHD diagnostic biomarkers, hepatocyte growth factor (HGF) and cytokeratin fragment 18, in 954 hematopoietic cell transplantation patients. All 3 biomarkers were significantly elevated in LGI GVHD compared with non-GVHD diarrhea; REG3α discerned LGI GVHD from non-GVHD diarrhea better than HGF and cytokeratin fragment 18. Although all 3 biomarkers predicted nonresponse to therapy at day 28 in LGI GVHD patients, only REG3α and HGF concentrations predicted 1-year nonrelapse mortality ($P = .01$ and $P = .02$, respectively). Liver GVHD without GI involvement at GVHD onset and non-GVHD liver complications were uncommon; all 3 biomarkers were elevated in liver GVHD, but did not distinguish GVHD from other causes of hyperbilirubinemia. (*Blood.* 2012;119(12): 2960-2963)

Introduction

Acute GVHD, a leading cause of nonrelapse mortality (NRM) after allogeneic hematopoietic cell transplantation (HCT), is measured by dysfunction in the skin, liver, and gastrointestinal (GI) tract.[1-3] We recently identified regenerating islet-derived 3-α (REG3α), an antimicrobial protein expressed in Paneth cells, as a biomarker of GVHD of the lower GI (LGI) tract that can differentiate LGI GVHD from non-GVHD diarrhea. Concentrations of this biomarker at onset of GVHD can predict response to treatment and NRM.[4] Hepatocyte growth factor (HGF) has been reported as a biomarker that is elevated in GVHD of the GI tract and liver as part of a panel of 4 GVHD biomarkers.[5] Similarly, cytokeratin fragment 18 (KRT18), an apoptotic protein, was described previously as a biomarker of visceral GVHD in a cohort of 55 patients,[6] and has recently been correlated with response to GVHD therapy.[7] Liver involvement has been historically observed in up to 36% of GVHD patients,[8,9] although a recent cohort demonstrated a declining incidence.[10] Liver involvement at GVHD onset occurs in 6%-20% of patients[8,9,11] and has been associated with poor response to GVHD therapy and increased NRM.[8,9,12] There are no validated biomarkers specific to liver GVHD. We compared the diagnostic and prognostic utility of REG3α, HGF, and KRT18 for LGI and liver GVHD.

Methods

Patients and samples

All plasma/serum samples and patient information were collected after obtaining patient consent in accordance with the Declaration of Helsinki for institutional review board–approved studies at the University of Michigan (n = 826), Regensburg, Germany (n = 88), and Kyushu, Japan (n = 40) for patients receiving HCT between January 2000 and November 2010, as described previously (and see supplemental Methods, available on the *Blood* Web site; see the Supplemental Materials link at the top of the online article).[4] Patients were divided into 6 groups: (1) patients with newly diagnosed GVHD diarrhea with or without skin involvement but without liver involvement (LGI GVHD), (2) patients with diarrhea inconsistent with GVHD either by clinical or histologic criteria (non-GVHD diarrhea), (3) patients with liver GVHD with or without skin involvement but without GI involvement (liver GVHD), (4) patients with liver complications attributable to non-GVHD causes (non-GVHD liver), (5) patients who presented with isolated skin GVHD (skin GVHD), and (6) patients at similar time points who never developed GVHD symptoms (no GVHD). Patient numbers and characteristics are shown in Table 1 and in supplemental Methods. Non-GVHD liver complications were included if patients never developed acute GVHD and experienced hyperbilirubinemia within 120 days of HCT in the absence of chronic GVHD. Causes of non-GVHD diarrhea and liver complications are described in supplemental Table 1. All samples were obtained at GVHD onset within 48 hours of initiation of systemic GVHD therapy and 1 sample was analyzed per patient. Patients who had non-GVHD complications before GVHD onset had samples evaluated only at GVHD onset. The rare incidence of liver involvement at GVHD onset did not permit analysis of 2 independent validation sets as was performed for REG3α in LGI GVHD.[4]

ELISAs

KRT18 ELISA kits were purchased from Peviva AB (M30 Apoptosense ELISA) and performed according to manufacturer protocol. Samples (diluted 1:2) and standards were run in duplicate. Absorbance was measured with a SpectraMax M2 (Molecular Devices), and results were calculated with SoftMax Pro Version 5.4 software (Molecular Devices).

Submitted October 20, 2011; accepted January 23, 2012. Prepublished online as *Blood* First Edition paper, January 27, 2012; DOI 10.1182/blood-2011-10-387357.

The online version of this article contains a data supplement.

The publication costs of this article were defrayed in part by page charge payment. Therefore, and solely to indicate this fact, this article is hereby marked "advertisement" in accordance with 18 USC section 1734.

Table 1. HCT patient characteristics (N = 954)

	LGI GVHD (n = 144)†	Non-GVHD diarrhea (n = 42)	Liver GVHD (n = 16)†	Non-GVHD liver (n = 25)	Skin GVHD (n = 337)	No GVHD (n = 390)	*P*
Age, y							
Median (range)	52 (0-67)	46 (3-66)	44 (19-63)	35 (0-64)	48 (0-70)	46 (0-68)	.001
Disease							
Malignant	94% (n = 135)	86% (n = 36)	100% (n = 16)	80% (n = 20)	94% (n = 317)	88% (n = 342)	.005
Other	6% (n = 9)	14% (n = 6)	0% (n = 0)	20% (n = 5)	6% (n = 20)	12% (n = 48)	
Disease status at transplantation*							
Low-/intermediate-risk	59% (n = 79)	67% (n = 24)	44% (n = 7)	75% (n = 15)	65% (n = 205)	66% (n = 226)	.3
High-risk	41% (n = 56)	33% (n = 12)	56% (n = 9)	25% (n = 5)	35% (n = 112)	34% (n = 116)	
Donor type							
Related donor	42% (n = 60)	52% (n = 22)	56% (n = 9)	68% (n = 17)	37% (n = 124)	58% (n = 228)	< .001
Unrelated donor	58% (n = 84)	48% (n = 20)	44% (n = 7)	32% (n = 8)	63% (n = 213)	42% (n = 162)	
Donor match							
Matched donor	71% (n = 102)	93% (n = 39)	81% (n = 13)	88% (n = 22)	73% (n = 245)	89% (n = 346)	< .001
Mismatched donor	29% (n = 42)	7% (n = 3)	19% (n = 3)	12% (n = 3)	27% (n = 92)	11% (n = 44)	
Conditioning regimen intensity							
High-intensity	53% (n = 77)	64% (n = 27)	69% (n = 11)	84% (n = 21)	54% (n = 181)	61% (n = 239)	.02
Moderate-intensity	47% (n = 67)	36% (n =15)	31% (n = 5)	16% (n = 4)	46% (n = 156)	39% (n = 151)	
Grade of GVHD at onset							
Grade 0	0% (n = 0)	100% (n = 42)	0% (n = 0)	100% (n = 25)	0% (n = 0)	100% (n = 390)	
Grade I	0% (n = 0)	0% (n = 0)	0% (n = 0)	0% (n = 0)	69% (n = 231)	0% (n = 0)	
Isolated skin stage 1	0% (n = 0)	0% (n = 0)	0% (n = 0)	0% (n = 0)	38% (n = 129)	0% (n = 0)	
Isolated skin stage 2	0% (n = 0)	0% (n = 0)	0% (n = 0)	0% (n = 0)	30% (n = 102)	0% (n = 0)	
Grade II	52% (n = 75)	0% (n = 0)	44% (n = 7)	0% (n = 0)	31% (n = 105)	0% (n = 0)	
Isolated skin stage 3	0% (n = 0)	0% (n = 0)	0% (n = 0)	0% (n = 0)	31% (n = 105)	0% (n = 0)	
GI or liver stage 1	52% (n = 75)†	0% (n = 0)	44% (n = 7)	0% (n = 0)	0% (n = 0)	0% (n = 0)	
Grade III-IV	48% (n = 69)	0% (n = 0)	56% (n = 9)	0% (n = 0)	< 1% (n = 1)	0% (n = 0)	
Isolated skin stage 4	0% (n = 0)	0% (n = 0)	0% (n = 0)	0% (n = 0)	< 1% (n = 1)	0% (n = 0)	
GI or liver stage 2	17% (n = 24)†	0% (n = 0)	38% (n = 6)	0% (n = 0)	0% (n = 0)	0% (n = 0)	
GI or liver stage 3	18% (n = 26)†	0% (n = 0)	13% (n = 2)	0% (n = 0)	0% (n = 0)	0% (n = 0)	
GI or liver stage 4	13% (n = 19)†	0% (n = 0)	6% (n = 1)	0% (n = 0)	0% (n = 0)	0% (n = 0)	
Days after HCT							
Median (range)	30 (7-215)	21 (7-78)	33 (10-112)	21 (7-106)	28 (5-485)	30 (7-185)	< .001

*High risk of disease status at HCT is according to Center for International Blood and Marrow Transplant Research guidelines.
†With or without skin GVHD involvement.

Other biomarker ELISAs were performed as described previously (and see supplemental Methods).[4,5]

Statistical analysis

Biomarker concentrations from individual patient samples were compared using 2-sample *t* tests applied to log-transformed concentrations. Differences in characteristics between patient groups were assessed with a Kruskal-Wallis test for continuous values and χ^2 tests of association for categorical values. Receiver operating characteristic (ROC) areas under the curve (AUCs) were estimated nonparametrically. NRM was modeled with cumulative incidence regression methods as described by Fine and Gray.[13]

Results and discussion

Biomarker concentrations were measured in samples from N = 954 allogeneic HCT recipients from the University of Michigan (n = 826), University Medical Center Regensburg (n = 88), and Kyushu University (n = 40; Table 1). The incidence of liver involvement at onset of GVHD requiring systemic corticosteroids (35 of 285; 12%) in our patient dataset was comparable to previous reports.[8,9,11,14] There was no statistical difference in biomarker concentrations based on GVHD prophylaxis whether a calcineurin inhibitor was combined with either methotrexate or mycophenolate mofetil (supplemental Table 2). All 3 biomarkers were significantly elevated in LGI GVHD compared with non-GVHD diarrhea and asymptomatic patients (Figure 1A-C). REG3α and HGF concentrations were also elevated in LGI GVHD compared with isolated skin GVHD, whereas KRT18 concentrations were not. This is consistent with the KRT18 tissue expression profile,[15] but differs from findings reported by Luft et al that KRT18 concentrations are not elevated in skin GVHD.[6]

We compared the diagnostic ability of REG3α, HGF, and KRT18 as biomarkers for LGI GVHD using ROC curves. REG3α performed better than KRT18 and HGF as a diagnostic biomarker distinguishing LGI GVHD from non-GVHD diarrhea (Figure 1D; AUC = 0.79, 0.60, and 0.60, respectively). The combination of all 3 biomarkers into a composite panel provided minimal additional diagnostic utility to that of REG3α alone (AUC = 0.80). Positive and negative predictive values for diagnostic utility of all 3 biomarkers are listed in supplemental Table 3. REG3α concentrations maintained diagnostic utility in patients experiencing diarrhea within 14 days of HCT, whereas HGF and KRT18 did not (supplemental Table 4). All 3 biomarkers, when measured at the onset of LGI GVHD, predicted nonresponse to therapy at 28 days[16-18] (supplemental Figure 1 and supplemental Table 5).

We divided patients into groups of equal size according to whether biomarker concentrations were above (high) or below (low) the median concentration at the onset of LGI GVHD. High REG3α and HGF concentrations correlated with significantly higher 1-year NRM, whereas there was no significant correlation

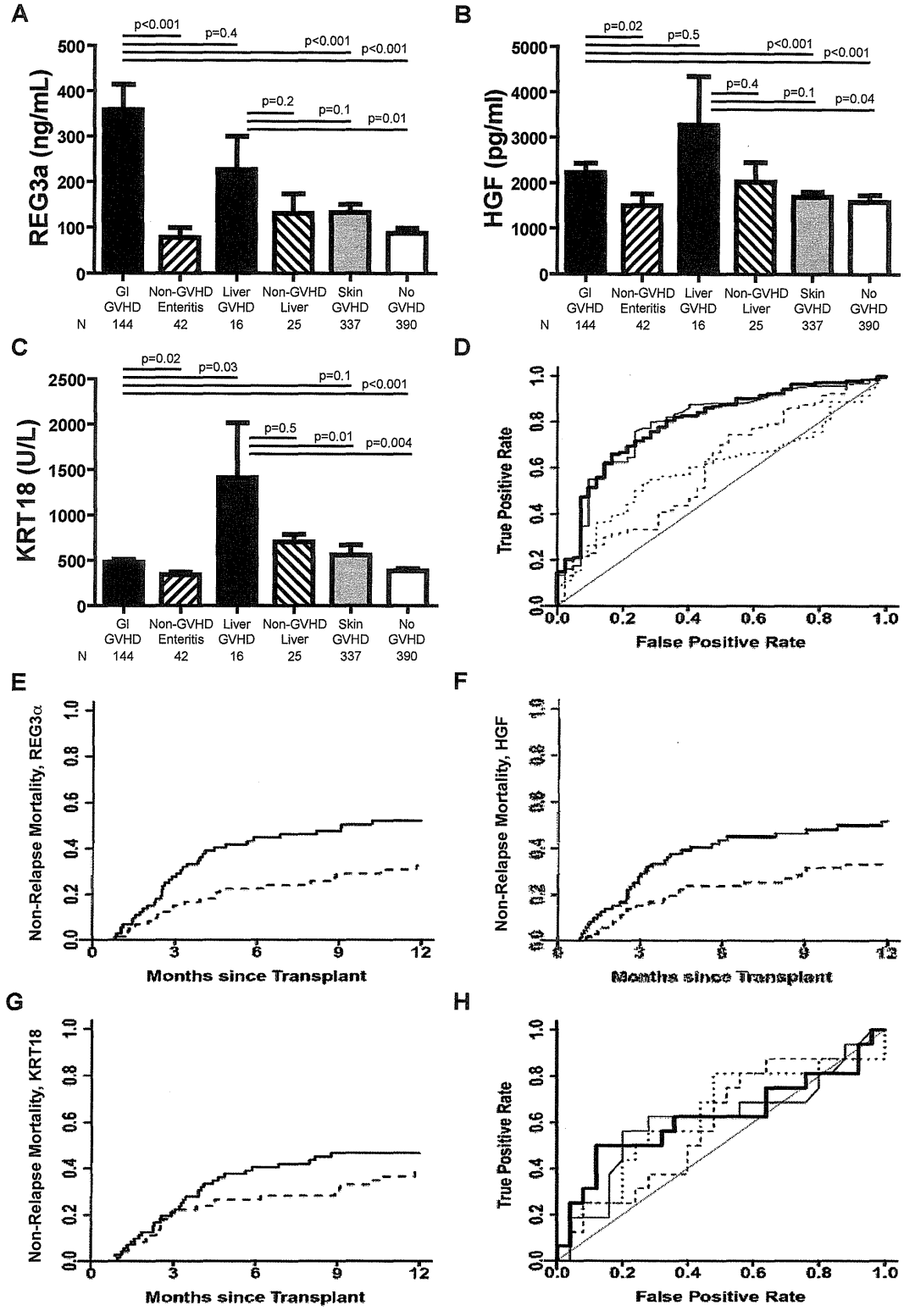

Figure 1. Biomarkers at the onset of GVHD symptoms. (A-C) REG3α, HGF, and KRT18 concentrations, respectively, at the onset of symptoms consistent with GVHD in 954 HCT patients. (D) ROC curves comparing biomarker concentrations at the onset of LGI GVHD without liver GVHD (n = 144) and non-GVHD diarrhea (n = 42). REG3α (thin solid line): AUC = 0.79; HGF (dotted line): AUC = 0.60; KRT18 (dashed line): AUC = 0.60; composite of all 3 biomarkers (thick solid line): AUC = 0.80. (E-G) NRM in patients with LGI GVHD at onset with onset concentrations above the median (solid line; n = 89) versus patients with onset concentrations below the median (dotted line; n = 89) for REG3a, HGF, and KRT18, respectively. (E) REG3a: > 135 ng/mL versus ≤ 135 ng/mL; 52% versus 33%, $P = .01$. (F) HGF: > 1398 pg/mL versus ≤ 1398 pg/mL; 52% versus 33%, $P = .02$. (G) KRT18 > 373 U/L versus ≤ 373 U/L; 47% versus 38%, $P = .3$. (H) ROC curves comparing biomarker concentrations at the onset of liver GVHD without GI GVHD (n = 16) and non-GVHD liver complications (n = 25); REG3α (thin solid line): AUC = 0.61; HGF (dotted line): AUC = 0.59; KRT18 (dashed line): AUC = 0.63; composite of all 3 biomarkers (thick solid line): AUC = 0.62.

between NRM and high KRT18 concentrations. (Figure 1E-G; $P = .01$, $P = .02$, and $P = .3$, respectively). Biomarker concentrations were comparable at onset between patients receiving systemic corticosteroids alone (n = 102) and those receiving multiagent therapy (n = 40) as initial GVHD treatment (supplemental Table 6).

In the present study and as reported recently,[10] liver GVHD without GI involvement at the onset of disease was uncommon (n = 16; 3% of GVHD patients and 2% of all patients), as were liver complications early after HCT (n = 25; 3% of all patients). REG3α and HGF concentrations were elevated in liver GVHD compared with asymptomatic patients, but were comparable to concentrations in patients with LGI GVHD, non-GVHD hyperbilirubinemia, and isolated skin GVHD (Figure 1A-B). KRT18 concentrations were significantly higher in patients with liver GVHD than in all other patients except those with non-GVHD liver complications (Figure 1C). None of the 3 biomarkers effectively distinguished liver GVHD from non-GVHD liver complications (Figure 1H; AUC = 0.61, 0.59, and 0.63, respectively; composite panel AUC = 0.62). Most patients with non-GVHD liver complications had sinusoidal obstruction syndrome (n = 20), which can often be distinguished clinically from GVHD. Cases in which biopsies were required to determine the etiology of hyperbilirubinemia during the period in which patients typically develop acute GVHD were very uncommon in our patient cohort (n = 7).

When including all patients with concomitant GI and liver involvement at GVHD onset regardless of other organ involvement (n = 35), REG3α concentrations at the onset of liver GVHD were significantly higher than concentrations at onset of non-GVHD hyperbilirubinemia (supplemental Figure 2). Comparing concentrations from all 35 liver GVHD patients with those from the 25 patients with non-GVHD liver complications, the AUC of the REG3α ROC curve improved to 0.69, whereas curves for KRT18 and HGF performed more poorly (0.54 and 0.57, respectively), reinforcing the strength of REG3α as an LGI GVHD biomarker and lack of specificity of KRT18 and HGF as visceral GVHD biomarkers.

In conclusion, REG3α performs better than HGF and KRT18 as a diagnostic biomarker of LGI GVHD. All 3 biomarkers predicted day 28 nonresponse to therapy, and both REG3α and HGF are good prognostic markers for 1-year NRM in patients with LGI GVHD. These findings should be validated in a prospective, multicenter study. Hyperbilirubinemia was an uncommon occurrence in our patient cohort, and the preliminary findings from this study warrant further investigation. In addition, a dedicated proteomics search should be performed to identify potential biomarkers specific to liver GVHD pathophysiology. This search should then be validated in a multicenter trial because of the rarity of this post-HCT complication and to minimize any potential center effect.

Acknowledgments

This study was supported by grants from the National Institutes of Health (RC1-HL-101102, P01-CA039542, and T32-HL007622), the Hartwell Foundation, and the Doris Duke Charitable Foundation. J.L.M.F. is a clinical research professor of the American Cancer Society and a visiting fellow of the Oxford All Souls College. S.P. is an investigator of the Eric Hartwell fund and the Amy Strelzer Manasevit Research Program.

Authorship

Contribution: A.C.H. designed and planned the experiments, performed the research, performed the data collection and quality assurance, analyzed the data, and wrote the manuscript; J.L.M.F. planned the study, interpreted the data, and wrote the manuscript; T.M.B. was the study statistician and wrote the manuscript; E.H., T.T., J.E.L., S.W.C, K.L., K.A., D.R.C., and P.R. contributed to patient accrual, clinical data collection, and quality assurance, to discussions of the research, and to writing of the manuscript; M.V.L. performed the experiments and wrote the manuscript; and S.P. conceived and planned the study design, performed the experiments, interpreted the data, and wrote the manuscript.

Conflict-of-interest disclosure: The authors declare no competing financial interests.

Correspondence: Dr Sophie Paczesny, Blood and Marrow Transplant Program, University of Michigan Comprehensive Cancer Center, Room 6410, 1500 E Medical Center Dr, Ann Arbor, MI, 48109-5942; e-mail: sophiep@med.umich.edu.

References

1. Cutler C, Antin JH. Manifestation and treatment of acute graft-versus-host-disease. In: Appelbaum F, Forman SJ, Negrin RS, Blume KG, eds. *Thomas' Hematopoietic Cell Transplantation*. 4th Ed. London, United Kingdom: Blackwell Publishing; 2009:1287-1303.
2. Ferrara JL, Levine JE, Reddy P, Holler E. Graft-versus-host disease. *Lancet*. 2009;373:1550-1561.
3. Welniak LA, Blazar BR, Murphy WJ. Immunobiology of allogeneic hematopoietic stem cell transplantation. *Annu Rev Immunol*. 2007;25:139-170.
4. Ferrara JL, Harris AC, Greenson JK, et al. Regenerating islet-derived 3 alpha is a biomarker of gastrointestinal graft-versus-host disease. *Blood*. 2011;118(25):6702-6708.
5. Paczesny S, Krijanovski OI, Braun TM, et al. A biomarker panel for acute graft-versus-host disease. *Blood*. 2009;113(2):273-278.
6. Luft T, Conzelmann M, Benner A, et al. Serum cytokeratin-18 fragments as quantitative markers of epithelial apoptosis in liver and intestinal graft-versus-host disease. *Blood*. 2007;110(13):4535-4542.
7. Luft T, Dietrich S, Falk C, et al. Steroid-refractory GVHD: T-cell attack within a vulnerable endothelial system. *Blood*. 2011;118(6):1685-1692.
8. Lee KH, Choi SJ, Lee JH, et al. Prognostic factors identifiable at the time of onset of acute graft-versus-host disease after allogeneic hematopoietic cell transplantation. *Haematologica*. 2005;90(7):939-948.
9. Robin M, Porcher R, de Castro R, et al. Initial liver involvement in acute GVHD is predictive for non-relapse mortality. *Transplantation*. 2009;88(9):1131-1136.
10. Gooley TA, Chien JW, Pergam SA, et al. Reduced mortality after allogeneic hematopoietic-cell transplantation. *N Engl J Med*. 2010;363(22):2091-2101.
11. MacMillan ML, Weisdorf DJ, Wagner JE, et al. Response of 443 patients to steroids as primary therapy for acute graft-versus-host disease: comparison of grading systems. *Biol Blood Marrow Transplant*. 2002;8(7):387-394.
12. Weisdorf D, Haake R, Blazar B, et al. Treatment of moderate/severe acute graft-versus-host disease after allogeneic bone marrow transplantation: an analysis of clinical risk features and outcome. *Blood*. 1990;75(4):1024-1030.
13. Fine JP, Gray RJ. A proportional hazards model for the subdistribution of a competing risk. *J Am Stat Assoc*. 1999;94:496-509.
14. Mielcarek M, Storer BE, Boeckh M, et al. Initial therapy of acute graft-versus-host disease with low-dose prednisone does not compromise patient outcomes. *Blood*. 2009;113(13):2888-2894.
15. Chu PG, Weiss LM. Keratin expression in human tissues and neoplasms. *Histopathology*. 2002;40(5):403-439.
16. MacMillan ML, DeFor TE, Weisdorf DJ. The best endpoint for acute GVHD treatment trials. *Blood*. 2010;115(26):5412-5417.
17. Levine JE, Logan B, Wu J, et al. Graft-versus-host disease treatment: predictors of survival. *Biol Blood Marrow Transplant*. 2010;16(12):1693-1699.
18. Saliba RM, Couriel DR, Giralt S, et al. Prognostic value of response after upfront therapy for acute GVHD. *Bone Marrow Transplant*. 2012;47(1):125-131.

CIN85 is required for Cbl-mediated regulation of antigen receptor signaling in human B cells

Hiroaki Niiro,[1] Siamak Jabbarzadeh-Tabrizi,[1] Yoshikane Kikushige,[2] Takahiro Shima,[1] Kumiko Noda,[1] Shun-ichiro Ota,[1] Hirofumi Tsuzuki,[1] Yasushi Inoue,[1] Yojiro Arinobu,[2] Hiromi Iwasaki,[2] Shinji Shimoda,[1] Eishi Baba,[1] Hiroshi Tsukamoto,[1] Takahiko Horiuchi,[1] Tadayoshi Taniyama,[3] and Koichi Akashi[1]

[1]Department of Medicine and Biosystemic Science, Graduate School of Medical Sciences, Kyushu University, Fukuoka, Japan; [2]Center for Cellular and Molecular Medicine, Kyushu University Hospital, Fukuoka, Japan; and [3]Laboratory of Bacterial Infection and Immunity, Department of Immunology, National Institute of Infectious Diseases, Tokyo, Japan

The aberrant regulation of B-cell receptor (BCR) signaling allows unwanted B cells to persist, thereby potentially leading to autoimmunity and B-cell malignancies. Casitas B-lineage lymphoma (Cbl) proteins suppress BCR signaling; however, the molecular mechanisms that control Cbl function in human B cells remain unclear. Here, we demonstrate that CIN85 (c-Cbl interacting protein of 85 kDa) is constitutively associated with c-Cbl, Cbl-b, and B-cell linker in B cells. Experiments using CIN85-overexpressing and CIN85-knockdown B-cell lines revealed that CIN85 increased c-Cbl phosphorylation and inhibited BCR-induced calcium flux and phosphorylation of Syk and PLCγ2, whereas it did not affect BCR internalization. The Syk phosphorylation in CIN85-overexpressing and CIN85-knockdown cells was inversely correlated with the ubiquitination and degradation of Syk. Moreover, CIN85 knockdown in primary B cells enhanced BCR-induced survival and growth, and increased the expression of BcLxL, A1, cyclin D2, and myc. Following the stimulation of BCR and Toll-like receptor 9, B-cell differentiation-associated molecules were up-regulated in CIN85-knockdown cells. Together, these results suggest that CIN85 is required for Cbl-mediated regulation of BCR signaling and for downstream events such as survival, growth, and differentiation of human B cells. (*Blood*. 2012;119(10):2263-2273)

Introduction

B-cell receptor (BCR) signaling guides critical cell fate decisions in B cells during ontogeny.[1,2] BCRs can generate tolerogenic signals to purge or silence B cells that bind to self-antigens, and immunogenic signals to expand B cells that are specific for foreign antigens. Thus, BCR signaling must be properly regulated at the various stages of B-cell development, as aberrant regulation of BCR signaling potentially leads to autoimmunity and B-cell malignancies.

On BCR ligation by antigens, the Src-family protein tyrosine kinase (PTK) Lyn and Syk are initially activated. Syk propagates the signal by phosphorylating downstream signaling molecules, causing the activation of critical signaling intermediates phosphoinositol 3-kinase (PI3K) and phospholipase C (PLC)γ2. PI3K activates Akt kinase, which is important for B-cell survival.[3] PLCγ2 activation induces the release of intracellular Ca^{2+} and the activation of protein kinase C (PKC), which cause the activation of mitogen-activated protein kinases (MAPKs; ERK, JNK, and p38 MAPK) and of transcription factors, including NF-κB and NF-AT. These molecules regulate further downstream molecules that are responsible for determining B-cell fates such as survival, growth, and differentiation.[1,2]

Casitas B-lineage lymphoma (Cbl) proteins are E3 ubiquitin ligases that regulate signals of various receptors by promoting the ubiquitination of signaling components.[4,5] Tyrosine phosphorylation of Cbl proteins is critical for their function.[6] Mammalian Cbl proteins consist of 3 members, c-Cbl, Cbl-b, and Cbl-3, among which c-Cbl and Cbl-b are expressed in hematopoietic cells.[7] In B cells, Cbl proteins associate with Syk and B-cell linker (BLNK), and negatively regulate BCR signaling.[8,9] B cell-specific ablation of c-Cbl/Cbl-b proteins in mice causes aberrant BCR signaling as well as impaired B-cell anergy, culminating in the development of systemic lupus erythematosus (SLE)–like disease.[10] In addition, c-Cbl is hypophosphorylated on tyrosine in advanced stages of chronic lymphocytic leukemia (CLL).[11] These findings suggest that Cbl-mediated regulation of BCR signaling is critical for the fate decisions of self-reactive and malignant B cells.

Adaptors are noncatalytic molecules that integrate the spatial and temporal assembly of multiprotein complexes involved in the survival, growth, and differentiation of B cells. We previously showed that the B lymphocyte adaptor molecule of 32 kDa (Bam32)/DAPP1 regulates BCR signaling/internalization and B-cell survival.[12,13] The *SH3KBP1* (SH3-domain kinase-binding protein 1) gene, which is also known as CIN85 (c-Cbl interacting protein of 85 kDa), encodes an adaptor that is independently identified by several groups and contains 3 SH3 domains, a proline-rich region, and a coiled-coil domain.[14-17] Early studies showed that in nonimmune cells, CIN85 regulates the clathrin-dependent internalization of receptor tyrosine kinases (RTKs) such as epidermal growth factor receptors (EGFRs).[18,19] The formation of the ternary complex of CIN85, c-Cbl, and endophillin is critical for this process. In immune cells, however, little is known approximately the function of CIN85. CIN85 facilitates ligand-induced FcεRI internalization in RBL-2H3 mast cells.[20] In addition, it regulates FcεRI signaling via Cbl-mediated regulation of

Submitted April 29, 2011; accepted January 13, 2012. Prepublished online as *Blood* First Edition paper, January 18, 2012; DOI 10.1182/blood-2011-04-351965.

The online version of this article contains a data supplement.

The publication costs of this article were defrayed in part by page charge payment. Therefore, and solely to indicate this fact, this article is hereby marked "advertisement" in accordance with 18 USC section 1734.

Syk expression in RBL-2H3 cells.[21] A recent study showed that CIN85 modulates c-Cbl–mediated down-regulation of FcγRIIa in human neutrophils.[22] It is thus of interest to determine whether CIN85 regulates the signaling pathways of other multimeric immune receptors, such as the T- and B-cell receptors.

Here, we demonstrate that CIN85 is constitutively associated with c-Cbl, Cbl-b, and BLNK in human B cells. Gain-of-function and loss-of-function experiments revealed that CIN85 up-regulated c-Cbl phosphorylation and inhibited BCR-induced calcium flux and phosphorylation of Syk and PLCγ2, without affecting BCR internalization. CIN85 also promoted c-Cbl–dependent ubiquitination and degradation of Syk. Moreover, CIN85 knockdown in primary B cells caused enhanced BCR-induced survival and growth, and augmented BCR/TLR9-induced expression of B-cell differentiation-associated molecules. Collectively, these results suggest that CIN85 is required for Cbl-mediated regulation of BCR signaling and for downstream events such as the survival, growth, and differentiation of human B cells.

Methods

Reagents

Goat anti–human IgM and IgG/IgA/IgM F(ab′)$_2$ fragments were purchased from Jackson ImmunoResearch Laboratories. Rabbit anti–human phospho-Zap-70 (Y319)/Syk (Y352), anti–human phospho-PLCγ2 (Y1217), anti–human phospho-Akt, anti–mouse Akt, anti–human phospho-JNK, anti–human phospho-ERK, and anti–human PLCγ2 pAbs as well as anti–human BclxL and Blimp-1 mAbs were purchased from Cell Signaling Technology. Mouse anti–human phospho-Btk, anti–human phospho-BLNK, anti–human c-Cbl, and anti–human Rac1 mAbs were from BD Immunocytometry. Mouse anti–human Cbl-b, anti–human Syk (4D10), anti–human BLNK, and anti-ubiquitin mAbs as well as rabbit anti–human c-Cbl and anti–mouse cyclin D2 pAbs were from Santa Cruz Biotechnology. Mouse anti-V5 mAb was from Invitrogen. Mouse anti-phosphotyrosine and anti–human CIN85 mAbs were from Upstate Biotechnology. Rabbit anti–human Vav2 mAb was from Epitomics. Sheep anti–human CD2AP pAb was from R&D Systems. Mouse anti–β-actin mAb was from Sigma-Aldrich.

B cell lines and primary B cells

The B lymphoma cell line BJAB was cultured in RPMI 1640 medium supplemented with 10% FCS. Human peripheral blood mononuclear cells, kindly provided by healthy volunteers, were separated from their buffy coats. Informed consent was obtained from all subjects in accordance with the Declaration of Helsinki. The Institutional Review Board of Kyushu University Hospital approved all research on human subjects. B cells were isolated with Dynabeads M450 CD19 and DETACHaBEAD CD19 (Dynal Biotech), according to the manufacturer's instructions. The isolated B cells exhibited greater than 99.5% viability on trypan blue exclusion and more than 95% purity on flow cytometry. Trace levels of phosphorylation of BCR-signaling molecules were observed in the B cells immediately after purification, probably because of mechanical stress.[23] The cells were thus rested for a couple of hours before further analysis. The cells were cultured at a density of 1×10^6 cells/mL in a 96 flat-bottom microtiter plate in complete RPMI 1640 medium supplemented with 10% FCS.

Expression constructs and transfection

Constructs encoding V5-tagged wild-type (WT) and 3 SH3 domain-deleted mutants of human CIN85 (pEF1/V5-CIN85 and –CIN85-dSH3ABC) were previously described.[24] The BJAB cells were transfected with the aforementioned constructs using a Gene Pulser apparatus (Bio-Rad Laboratories). The control cells were transfected with an empty vector. Stably transfected BJAB clones were selected in the presence of G418 (2 mg/mL) and screened with anti-V5 mAb.

RNA interference

The pSUPER-based strategy was adopted to knockdown hCIN85 expression. To generate CIN85 small-hairpin RNA (shRNA), a 19-nucleotide sequence (CAGCAATGACATTGACTTA) selected from human CIN85 cDNA was annealed and ligated into the pSUPER or GFP-pSUPER vector. A scrambled sequence (GTTACTAACGCGAATTAAC) was used as negative control. hCIN85 or the control shRNA vector was transfected into BJAB cells using a Gene Pulser apparatus, and stable hCIN85-knockdown BJAB clones were selected in the presence of puromycin (0.5 μg/mL). Transient transfections of primary B cells with the pSUPER-hCIN85 vector were performed using the Nucleofection kit from AMAXA Biosystems as previously described.[23]

Measurement of intracellular free calcium

B cells were washed with RPMI 1640 medium containing 10% FCS and adjusted to a concentration of 1×10^6 cells/mL. After incubation at 37°C for 15 minutes, 1 μg/mL of Fluo 4/AM (Dojindo) was added, and the cells were incubated for an additional 30 to 45 minutes with resuspension every 15 minutes. The cells were centrifuged and resuspended in RPMI 1640 at a density of 2×10^6 cells/mL and stimulated with anti-IgM (20 μg/mL). The fluorescence intensity of intracellular Fluo 4 was monitored and analyzed using flow cytometry.

Immunoprecipitation

Cells were lysed as described.[13] Subsequently, protein G-Sepharose (Amersham Pharmacia Biotech) precleared lysates were incubated with anti-V5, -BLNK, -Syk, -Cbl, -Vav2 mAb, or -CD2AP pAb for 1 hour at 4°C and then immunoprecipitated with protein G-Sepharose overnight at 4°C. The precipitated proteins were resolved by 10% SDS-PAGE; transferred onto a Millipore Immobilon polyvinylidene difluoride membrane; and blotted with anti-phosphotyrosine (4G10), -V5, -c-Cbl, -Cbl-b, -BLNK, -Vav2, -Syk, or -ubiquitin mAbs, followed by incubation with secondary HRP-conjugated IgG (Jackson ImmunoResearch Laboratories) specific for the primary Ab. The blots were developed with an ECL Plus kit (Amersham Biosciences).

Western blot analysis

Nonstimulated or stimulated cells (1×10^6) were lysed as described.[12] The lysates were then denatured in an equal volume of 2 × SDS sample buffer, resolved on a 10% SDS-PAGE gel, and electro-transferred to nitrocellulose membranes in non-SDS–containing transfer buffer (25mM Tris, 0.2M glycine, and 20% methanol; pH 8.5). Western blotting was performed with anti–phospho-Syk (1:2000), anti–phospho-PLCγ2 (1:2000), anti–phospho-BLNK (1:2000), anti–phospho-JNK (1:2000), anti–phospho-ERK (1:2000), anti–phospho-Akt (1:2000), anti-Akt (1:2000), anti-CIN85 (1:2000), anti–β-actin (1:2000), or anti-Vav2 (1:2000), followed by a 1:15 000 dilution of anti–rabbit or anti–mouse HRP-conjugated IgG. The blots were developed with the ECL plus kit (Amersham Biosciences). The chemiluminescence intensity was monitored using a Laser3000 (FujiFilm) instrument. We quantitated the band intensity of the proteins using ImageGauge Version 4.22 software (FujiFilm). The resulting values were expressed as fold changes in protein expression relative to the protein expression in unstimulated control cells.

Luciferase assays

Cells (1×10^7) were transfected by electroporation with the NF-AT-reporter construct, which was generously provided by Dr Shoichiro Miyatake (The Tokyo Metropolitan Institute of Medical Science, Tokyo, Japan). After 18 to 20 hours, cells were harvested and plated on 96-well plates at a density of 2×10^5/well. Triplicate cultures were incubated in the media alone with graded doses of anti-IgM or with 50nM PMA and 2.5μM ionomycin. After 6 hours, the cells were lysed in 50 μL reporter lysis buffer (Promega) for 15 minutes at room temperature. The luciferase activity was assayed by adding 20 μL luciferase substrate (Promega) to 50 μL lysate

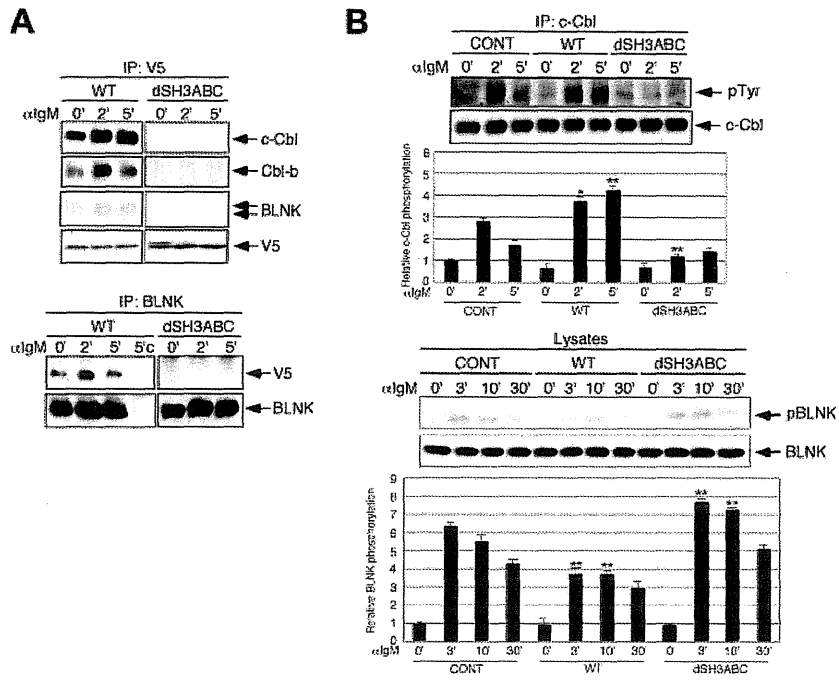

Figure 1. CIN85 associates with Cbl and BLNK and regulates their phosphorylation in B cells. (A) BJAB cells stably expressing either WT or SH3-deleted CIN85 were stimulated with 20 μg/mL of F(ab') 2 goat anti–human IgM for the indicated time periods. Immunoprecipitates with anti-V5 or anti-BLNK mAb were separated on a 10% SDS-PAGE gel and analyzed by Western blotting with anti–c-Cbl, anti–Cbl-b, anti-BLNK, or anti-V5 mAb. 5′c, immunoprecipitation of the cell lysates at 5 minutes with isotype control. (B) Control BJAB cells and stable transformants expressing either WT or SH3-deleted CIN85 were stimulated with 20 μg/mL of F(ab') 2 goat anti–human IgM for the indicated time periods. Immunoprecipitates with anti–c-Cbl mAb were separated on a 10% SDS-PAGE gel and analyzed by Western blotting with anti-phosphotyrosine or anti–c-Cbl mAb. The resulting values are expressed as fold changes in protein expression compared with unstimulated control cells. The values are the mean ± SD of 3 independent experiments (*$P < .05$, **$P < .01$ vs controls). (C) Control BJAB cells and stable transformants expressing either WT or SH3-deleted CIN85 were stimulated with 20 μg/mL of F(ab') 2 goat anti–human IgM for the indicated time periods. The cell lysates were subsequently separated on a 10% SDS-PAGE gel and analyzed by Western blotting with anti–phospho-BLNK or anti-BLNK mAb. The resulting values are expressed as fold changes in protein expression compared with unstimulated control cells. The values are the mean ± SD of 3 independent experiments (**$P < .01$ vs controls).

and immediately measuring the luminescence on a Lumat LB9507 luminometer (EG & G Berthold). To serve as a control for the transfection efficiency, the relative luciferase activity of the medium and cells stimulated with BCR was calculated relative to stimulation with PMA/ionomycin.

Flow cytometric analysis

BJAB cells were incubated on ice for 15 minutes with 20 μg/mL goat-unlabeled anti-IgM before they were washed with ice-cold medium and warmed at 37°C for the indicated time intervals. The cells were washed with ice-cold PBS containing 2% FBS and 0.2% sodium azide (Fisher Scientific) to stop internalization at the assigned time points and to remove the unbound Ab. The remaining surface BCRs were stained with FITC-labeled rabbit anti–goat Ig and quantified by flow cytometry. The data are presented as the percentage of surface BCR remaining.

Fluorescence microscopic analysis

BJAB cells were incubated with 10 μg/mL of unlabeled goat anti–human IgM sera (20 μg/mL) at 4°C for 30 minutes and warmed to 37°C for the indicated time periods. The cells were then fixed with 3.7% paraformaldehyde and permeabilized with PBS containing 1% BSA and 0.05% saponin (wash buffer). The cells were then incubated for 30 minutes with FITC-conjugated anti–goat IgG pAb (Jackson ImmunoResearch Laboratories) at 4°C. The stained cells were centrifuged onto slides and analyzed with inverted fluorescent microscopy (BZ-9000; Keyence).

Quantitative real-time PCR

The total RNA was extracted from the primary B cells using Isogen reagent (Nippon gene) and was treated with DNase I (Invitrogen) to remove contaminating genomic DNA. First-strand cDNA was synthesized using a QuantiTect reverse transcription kit (QIAGEN). Quantitative real-time PCR was performed in the ABI Prism 7700 Sequence Detector (Applied Biosystems). The reactions were performed in triplicate wells in 96-well plates. TaqMan target mixes for Cyclin D2, Myc, *BCL2L1*/BclxL, *BCL2A1*/A1, *PRDM1*/Blimp-1, and *XBP1* were purchased from Applied Biosystems. 18S ribosomal RNA (rRNA) was separately amplified in the same plate as an internal control for variation in the amount of cDNA in PCR. The collected data were analyzed using the Sequence Detector software (Applied Biosystems). The data were expressed as the fold change in gene expression relative to the expression in the control cells.

Annexin V staining

After culture, cells (1-2 × 10^5) were washed twice with PBS and suspended in 85 μL binding buffer (MBL) containing Ca^{2+}. The cell suspension supplemented with 10 μL annexin-V–FITC or annexin-V–PE (MBL) and 5 μg of propidium iodide (PI) or 1 μg of 7-ADD was incubated at room temperature for 15 minutes in the dark. Subsequently, binding buffer was added, and the fraction of early apoptotic cells was measured using flow cytometry.

BrdU assay

DNA synthesis was monitored by pulse-labeling cells for 2 hours with the thymidine analog 5-bromo-2′-deoxyuridine (BrdU). The cells were washed 3 times with PBS and fixed for 20 minutes at −20°C in an ethanol fixative (0.15mM glycine in 70% EtOH, pH 2.0). After rehydration in PBS, BrdU incorporation was detected by incubation with an anti-BrdU mAb for 1 hour at 37°C, followed by a rhodamine-conjugated anti–mouse antibody (1:500; Jackson ImmunoResearch Laboratories) and staining of the nucleus with 4′-6-diamidino-2-phenylindole for 1 hour. The proportion of BrdU-positive nuclei (BrdU labeling index) was assessed, based on a sample size of 500 cells per data point.

Statistical analysis

Statistical analysis was performed using the Student t test. $P < .05$ was considered statistically significant.

Results

CIN85 associates with Cbl and BLNK and regulates their phosphorylation

The tyrosine phosphorylation of signaling molecules is a critical event in BCR signaling.[1,2] Because SH3 domains play an important role in the function of CIN85,[25] we focused on

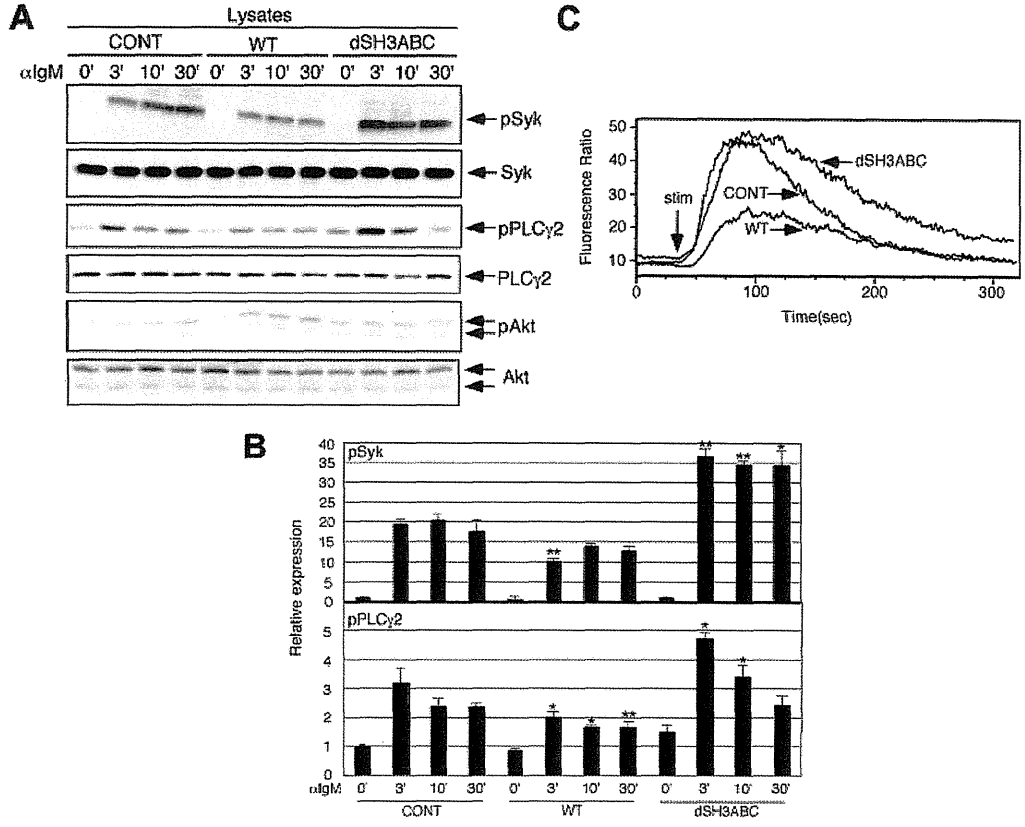

Figure 2. Forced CIN85 expression inhibits BCR-induced calcium flux and phosphorylation of Syk and PLCγ2. (A-B) Control BJAB cells and stable transformants expressing either WT or SH3-deleted CIN85 were stimulated with 20 μg/mL of $F(ab')_2$ goat anti–human IgM for the indicated time periods. The cell lysates were subsequently separated on a 10% SDS-PAGE gel and analyzed by Western blotting with anti–phospho-Syk pAb, anti-Syk mAb, anti–phospho-PLCγ2 pAb, anti-PLCγ2 pAb, anti–phospho-Akt pAb, or anti-Akt pAb. The resulting values are expressed as fold changes in protein expression compared with unstimulated control cells. The values are the mean ± SD of 3 independent experiments (*$P < .05$, **$P < .01$ vs controls). (C) Ca^{2+} influx in control BJAB cells and stable transformants expressing either WT or SH3-deleted CIN85. The intracellular free calcium levels in Fluo 4/AM-loaded cells were analyzed using flow cytometry after the cells were stimulated with 20 μg/mL $F(ab')_2$ goat anti–human IgM. The results shown are representative of 4 independent experiments.

tyrosine-phosphorylated molecules downstream of the BCR that could associate with the SH3 domains of CIN85. Specifically, we focused on the 2 molecules, BLNK and c-Cbl, that function as key positive and negative regulators of BCR signaling,[1,10] respectively; both proteins can associate with the SH3 domains of CIN85.[14,26]

We first determined the association of Cbl and BLNK with CIN85 using WT and SH3-deleted CIN85-expressing B cell lines. Consistent with previous reports,[14,26] WT CIN85 was constitutively associated with c-Cbl and BLNK, and these associations were increased after BCR stimulation (Figure 1A). Cbl-b was similarly associated with WT CIN85, albeit to a lesser extent. Although the association of WT CIN85 and BLNK appeared modest, the inverse immunoprecipitation of BLNK confirmed the association (Figure 1A). As expected, the association of Cbl and BLNK with CIN85 was abrogated in SH3-deleted CIN85-expressing B cells, suggesting that the SH3 domains of CIN85 are required for its association with Cbl and BLNK. Because the tyrosine phosphorylation of c-Cbl and BLNK is critical for their function,[6,27] we next determined whether the overexpression of WT and SH3-deleted CIN85 affects BCR-induced phosphorylation of c-Cbl and BLNK. Compared with control cells, WT and SH3-deleted CIN85 sustained and inhibited c-Cbl phosphorylation, respectively (Figure 1B). In addition, WT and SH3-deleted CIN85 inhibited and enhanced BLNK phosphorylation, respectively (Figure 1B). These findings suggest that CIN85 associates with Cbl and BLNK and regulates their phosphorylation in an opposite manner.

Forced CIN85 expression inhibits BCR-induced calcium flux and the phosphorylation of Syk and PLCγ2

We tested whether the overexpression of WT and SH3-deleted CIN85 affects early BCR signaling. Syk phosphorylation, which is one of the earliest events in BCR signaling, was inhibited in WT CIN85-expressing cells, whereas it was sustained in SH3-deleted CIN85-expressing cells (Figure 2A-B). Two enzymes, PLCγ2 and PI3K, function as critical mediators downstream of BCR signaling.[1,2,28] WT and SH3-deleted CIN85 partially inhibited and enhanced BCR-induced phosphorylation of PLCγ2, respectively (Figure 2A-B). In contrast, the phosphorylation of Akt, which is a downstream molecule of PI3K, was not affected in WT or SH3-deleted CIN85-expressing cells (Figure 2A). Activated PLCγ2 converts PIP2 into IP3 and diacyl glycerol, of which PIP2 is critical for calcium flux in B cells.[1,2,12] Consistent with the levels of PLCγ2 phosphorylation, the BCR-induced calcium flux was significantly inhibited in WT CIN85-expressing cells, whereas it was slightly sustained in SH3-deleted CIN85-expressing cells (Figure 2C). These results suggest that CIN85 inhibits BCR-induced calcium flux and the

phosphorylation of Syk and PLCγ2, and that the SH3 domains of CIN85 are required for its inhibitory function.

CIN85 knockdown enhances BCR-induced calcium flux and the phosphorylation of Syk, Vav2, and PLCγ2, leading to augmented NF-AT activation and CD69 expression

To elucidate the role of endogenously expressed CIN85 in BCR signaling, we generated CIN85-knockdown B cell lines. In contrast to the CIN85-overexpressing cells (Figures 1 and 2), CIN85-knockdown cells exhibited enhanced phosphorylation of Syk, BLNK, and PLCγ2 (Figure 3A-B). Akt phosphorylation was comparable between control and CIN85-knockdown cells (Figure 3A). Consistent with the levels of PLCγ2 phosphorylation, BCR-induced calcium flux was accentuated in CIN85-knockdown cells (Figure 3C). Vav2 positively regulates PLCγ2 activation in B cells.[29] Vav2 phosphorylation was enhanced in CIN85-knockdown cells (Figure 3D). These BCR signaling profiles in CIN85-knockdown cells are reminiscent of those in c-Cbl/Cbl-b double-knockout B cells.[10] The phosphorylation of c-Cbl was significantly inhibited in CIN85-knockdown cells (Figure 3E). BCR-induced calcium flux plays a crucial role in the activation of the transcription factor NF-AT, the disruption of which results in significant defects in B-cell function.[30] BCR-induced NF-AT activation was enhanced in CIN85-knockdown cells (Figure 3F). In addition, BCR-induced up-regulation of the activation marker CD69 was pronounced in CIN85-knockdown cells (Figure 3G). These phenotypes in CIN85-knockdown cells were again similar to those observed in Cbl-deficient B cells.[10] Given that CIN85 strongly associates with Cbl proteins (Figure 1A), these results suggest that CIN85 plays a vital role in Cbl-mediated regulation of BCR signaling.

CIN85 promotes the ubiquitination and degradation of Syk in B cells

Cbl proteins function as E3 ubiquitin ligases and target PTK substrates, including Syk, for degradation.[31,32] We thus tested whether CIN85 affects Syk ubiquitination in B cells. Syk ubiquitination was induced on BCR stimulation. Compared with control cells, Syk ubiquitination was increased in WT CIN85-expressing cells (Figure 4A). In contrast, an impairment in Syk ubiquitination was noted in CIN85-knockdown cells (Figure 4A). These results suggest that CIN85 positively regulates Cbl-mediated ubiquitination of BCR-signaling molecules including Syk. Despite the altered levels of Syk ubiquitination, the level of total Syk protein was not altered in the WT CIN85-expressing or CIN85-knockdown cells throughout the stimulation (Figures 2A and 3A). Because only a small pool of Syk is phosphorylated on stimulation and targeted for degradation in B cells,[31] we tested the degree of Syk phosphorylation among the total Syk immunoprecipitate. The levels of phosphorylated Syk were reduced in WT CIN85-expressing cells but enhanced in CIN85-knockdown cells (Figure 4B), suggesting that CIN85 promotes Cbl-dependent loss of the phosphorylated pool of Syk in B cells.

CIN85 does not affect BCR internalization

CIN85 regulates Cbl-mediated internalization of the EGFR in several cell types other than B cells.[18,19] To test whether CIN85 affects BCR internalization, we first monitored the levels of surface BCR expression after stimulation. Without stimuli, the levels of surface BCR were similar on CIN85 overexpression and CIN85 knockdown. In parental cells, BCR crosslinking caused a rapid decrease in surface BCR levels, suggesting that BCR was efficiently internalized after stimulation (Figure 5A; supplemental Figure 1A, available on the *Blood* Web site; see the Supplemental Materials link at the top of the online article). BCR internalization was not affected in the WT or SH3-deleted CIN85-expressing cells. Moreover, the absence of endogenous CIN85 did not affect BCR internalization (Figure 5B, supplemental Figure 1A). Next, we directly visualized BCRs in B cell lines using fluorescence microscopy. In control cells, the BCR complexes exhibited a slightly patchy distribution before stimulation, and within 3 minutes after stimulation, the BCRs formed polarized tight caps on the cell surface. After 10 minutes of BCR stimulation, a punctate pattern of internalized BCRs was clearly visualized (Figure 5C). Consistent with the findings obtained with flow cytometry (Figure 5A-B), the spatial and temporal distribution of BCR complexes in CIN85-overexpressing and CIN85-knockdown cells appeared similar to that in control cells (Figure 5C, supplemental Figure 1B-C). These findings suggest that CIN85 does not affect BCR internalization.

CIN85 knockdown enhances the survival, growth, and differentiation of primary B cells

BCR signaling plays a critical role in determining the survival, growth, and differentiation of B cells.[1] It was thus of interest to test whether CIN85 affects B cell fate. A major obstacle, however, is that the survival, growth, and differentiation of B cell cannot be properly assessed in transformed B cells. We therefore sought to knock down CIN85 expression in human primary B cells. After introduction of the GFP-CIN85 knockdown vector, GFP-positive B cells were sorted and used for further experimentation. Under these conditions, we were able to knock down the CIN85 mRNA expression in B cells by 60%-80% (Figure 6A).

We first tested whether CIN85 knockdown affects the expression of the B-cell survival-associated genes BcLxL and A1. Consistent with previous studies,[33] BCR stimulation induced BcLxL and A1 mRNA expression in control cells. This induction was far more drastic in CIN85-knockdown B cells (Figure 6A). The costimulation of TLR9 with its ligand CpG enhances BCR-induced expression of B-cell survival genes.[34] This enhancement was less evident in CIN85-knockdown cells than in control cells (Figure 6A), suggesting that CIN85 knockdown requires less costimulation for the full induction of B-cell survival genes. Consistent the findings for the transcript levels, the BCR-induced expression of BcLxL protein was more pronounced in CIN85-knockdown cells (Figure 6B). We also tested whether CIN85 knockdown affects BCR-induced death of B cells using the annexin-binding assay. The CIN85-knockdown cells exhibited less BCR-induced cell death (Figure 6C). We next tested whether CIN85 knockdown affects the expression of the B-cell growth-associated genes cyclin D2 and myc. Again, BCR-induced expression of these genes was more pronounced in CIN85-knockdown cells (Figure 6A), and costimulation with TLR9 did not enhance induction compared with the control cells. Consistent with the findings for the transcript levels, BCR-induced expression of cyclin D2 protein was more pronounced in CIN85-knockdown cells (Figure 6B). We also tested whether CIN85 knockdown affects B-cell growth using the BrdU uptake assay. Consistent with the expression levels of cyclin D2 and myc, CIN85 knockdown enhanced BCR-induced cell growth (Figure 6D). On activation, B cells undergo plasma cell differentiation along with the expression of critical differentiation-associated genes such as Blimp-1 and Xbp-1. Consistent with previous studies,[35] BCR stimulation alone was not sufficient to induce the expression of Blimp-1 and Xbp-1 in human B cells (data not shown). However, the combined stimulation of BCR and TLR9 clearly induced the expression of these genes in control cells,

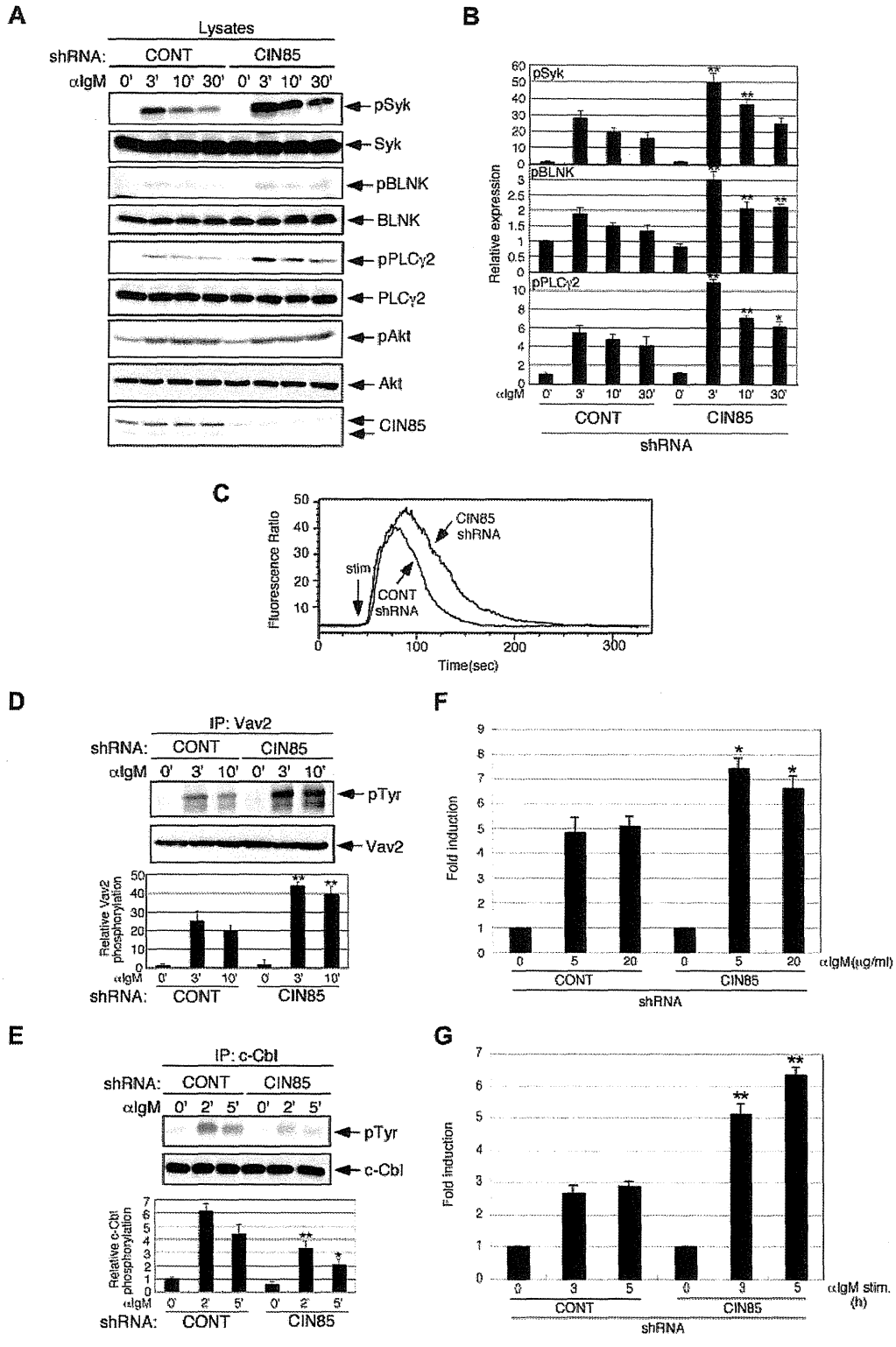

Figure 3. CIN85 knockdown enhances BCR-induced calcium flux and phosphorylation of Syk, Vav2, and PLCγ2, leading to augmented NF-AT activation and CD69 expression. (A-B) Stable control and CIN85-knockdown BJAB cells were stimulated with 20 μg/mL F(ab′) $_2$ goat anti–human IgM for the indicated time periods. The cell lysates were subsequently separated on a 10% SDS-PAGE gel and analyzed by Western blotting with anti–phospho-Syk pAb, anti-Syk mAb, anti–phospho-BLNK mAb, anti-BLNK mAb, anti–phospho-PLCγ2 pAb, anti-PLCγ2 pAb, anti–phospho-Akt pAb, anti-Akt pAb, or anti-CIN85 mAb. The resulting values are expressed as fold changes in protein expression compared with unstimulated control cells. The values are the mean ± SD of 3 independent experiments (*$P < .05$, **$P < .01$ vs controls). (C) Ca^{2+} influx in stable control and CIN85-knockdown BJAB cells. Intracellular free calcium levels in Fluo 4/AM-loaded cells were analyzed using flow cytometry after the cells were stimulated with 20 μg/mL F(ab′)$_2$ goat anti–human IgM. The results shown are representative of 4 independent experiments. (D-E) Stable control and CIN85-knockdown BJAB cells were stimulated with 20 μg/mL F(ab′)$_2$ goat anti–human IgM for the indicated time periods. Immunoprecipitates with anti-Vav2 or anti–c-Cbl mAb were separated on a 10% SDS-PAGE gel and analyzed by Western blotting with anti-phosphotyrosine mAb, anti-Vav2 mAb, or anti–c-Cbl mAb. The resulting values are expressed as fold changes in protein expression compared with unstimulated control cells. The values are the mean ± SD of 3 independent experiments (*$P < .05$, **$P < .01$ vs controls). (F) Stable control

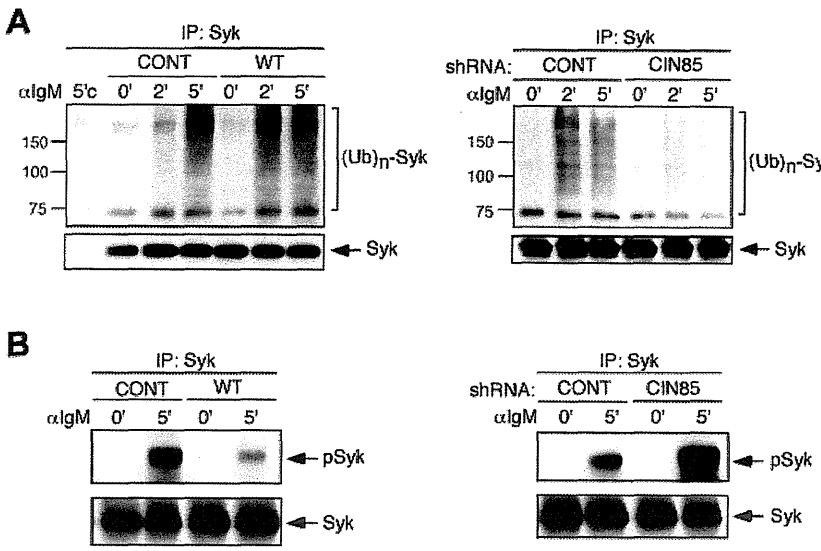

Figure 4. CIN85 promotes Syk ubiquitination and degradation in B cells. (A) Control BJAB cells, stable transformants expressing WT CIN85, and CIN85-knockdown BJAB cells were stimulated with 20 μg/mL $F(ab')_2$ goat anti–human IgM for the indicated time periods. Immunoprecipitates with anti-Syk mAb were separated on a 10% SDS-PAGE gel and analyzed by Western blotting with anti-ubiquitin or anti-Syk mAb. 5"c, immunoprecipitation of the cell lysates at 5 minutes with isotype control. The molecular weight is indicated on the left side of the blots. (B) Control BJAB cells, stable transformants expressing WT CIN85, and CIN85-knockdown BJAB cells were stimulated with 20 μg/mL $F(ab')_2$ goat anti–human IgM for 5 minutes. Immunoprecipitates with anti-Syk mAb were separated on a 10% SDS-PAGE gel and analyzed by Western blotting with anti–phospho-Syk pAb or anti-Syk mAb.

whereas this induction was more pronounced in CIN85-knockdown B cells (Figure 6E). Consistent with the findings for the transcript levels, BCR stimulation alone did not induce detectable levels of Blimp-1 protein. However, the combined stimulation of BCR and TLR9 clearly induced the expression of the Blimp-1 protein in control cells, although this was more pronounced in CIN85-knockdown cells (Figure 6F). These results suggest that CIN85 is required for Cbl-mediated regulation of BCR signaling and downstream events such as the survival, growth, and differentiation of human B cells.

Discussion

We demonstrated here that CIN85 functions as a novel adaptor to regulate proximal BCR signaling. Gain-of-function and loss-of-function experiments revealed that CIN85 not only enhances BCR-induced c-Cbl phosphorylation but also inhibits BCR-induced calcium flux and the phosphorylation of Syk and PLCγ2. CIN85 promotes c-Cbl–dependent ubiquitination and degradation of Syk, which is a key upstream kinase that propagates BCR signaling by phosphorylating downstream molecules including PLCγ2. Because Cbl proteins directly associate with Syk and inhibit its function,[6] it is probable that CIN85 acts as a critical scaffolding adaptor for Cbl proteins and is indispensable for Cbl-mediated regulation of Syk activation in B cells.

Consistent with our findings, a critical role of CIN85 in Cbl-mediated regulation of Syk activation was recently shown in FcεRI signaling in mast cells.[21] In mast cells, CIN85 enhances c-Cbl-mediated ubiquitination and the degradation of Syk protein.[21] In B cells, however, CIN85 overexpression significantly increased Syk ubiquitination (Figure 4), but CIN85 knockdown did not alter the total levels of Syk protein throughout stimulation (Figure 3A), as previously shown in c-Cbl/Cbl-b double-knockout B cells.[10] This apparent discrepancy in Syk degradation between mast cells and B cells could be explained by the findings of Rao et al,[31] who showed that on BCR stimulation, only a small portion of Syk is phosphorylated and then degraded by c-Cbl. Rao et al also showed that c-Cbl does not directly affect the catalytic activity of Syk.[31] Consistent with these findings, our study showed that CIN85 promotes c-Cbl–mediated ubiquitination and degradation of the phosphorylated pool of Syk (Figure 4A-B).

What, then, are the possible mechanisms by which CIN85 enhances BCR-induced c-Cbl phosphorylation in B cells? Src-family PTKs and Syk are proposed to phosphorylate c-Cbl on tyrosines.[6] We previously showed that CIN85 directly interacts with the SH3 domain of Src-family PTKs including Lyn.[17] In addition, CIN85 directly associates with BLNK, PLCγ and Vav, all of which are direct Syk interactors,[17,36] and thus, CIN85 is indirectly associated with Syk via binding to BLNK, PLCγ, and Vav. In view of these findings, it seems probable that CIN85 acts as a key scaffolding adaptor that permits the spatial proximity of Src-family PTKs, Syk, and Cbl proteins and thus facilitates their phosphorylation of Cbl proteins.

Although CIN85 appears to function in concert with Cbl proteins to regulate BCR signaling, an additional mechanism is possible. Previous in vitro binding experiments showed that CIN85 directly binds to Src-family tyrosine kinases, PLCγ, p85 PI3K,Vav, Btk, and SHIP, all of which are involved in BCR signaling, through its SH3 domains and proline-rich region.[15,24,25] In addition, a recent study showed that the SH3 domains of CIN85 could uniquely bind to ubiquitin.[37] Thus, after various BCR-signaling molecules are ubiquitinated by Cbl proteins on stimulation, the competition between canonical SH3 ligands and ubiquitin binding to CIN85 may affect BCR signaling in a temporal and spatial manner. Therefore, it is probable that CIN85 also directly regulates BCR signaling by a Cbl-independent mechanism.

A recent study using liquid chromatography-coupled tandem mass spectrometry showed that 3 SH3 domains of CIN85 could recruit protein molecules required for the proper formation and

Figure 3 (continued) and CIN85-knockdown BJAB cells transfected with the NF-AT luciferase reporter construct were stimulated with graded doses of $F(ab')_2$ goat anti–human IgM for 8 hours and lysed, and the luciferase activity was assayed using a luminometer. The relative luciferase activity of the medium and BCR-stimulated cells was expressed with respect to that of the PMA/ionomycin stimulation. The results were presented as the mean and SEM of triplicate cultures. One experiment representative of 4 independent experiments is shown (*$P < .05$ vs controls). (G) Stable control and CIN85-knockdown BJAB cells before and after stimulation with 20 μg/mL $F(ab')_2$ goat anti–human IgM (3 and 5 hours) were analyzed for surface expression of CD69. One experiment representative of 3 independent experiments is shown (**$P < .01$ vs controls).

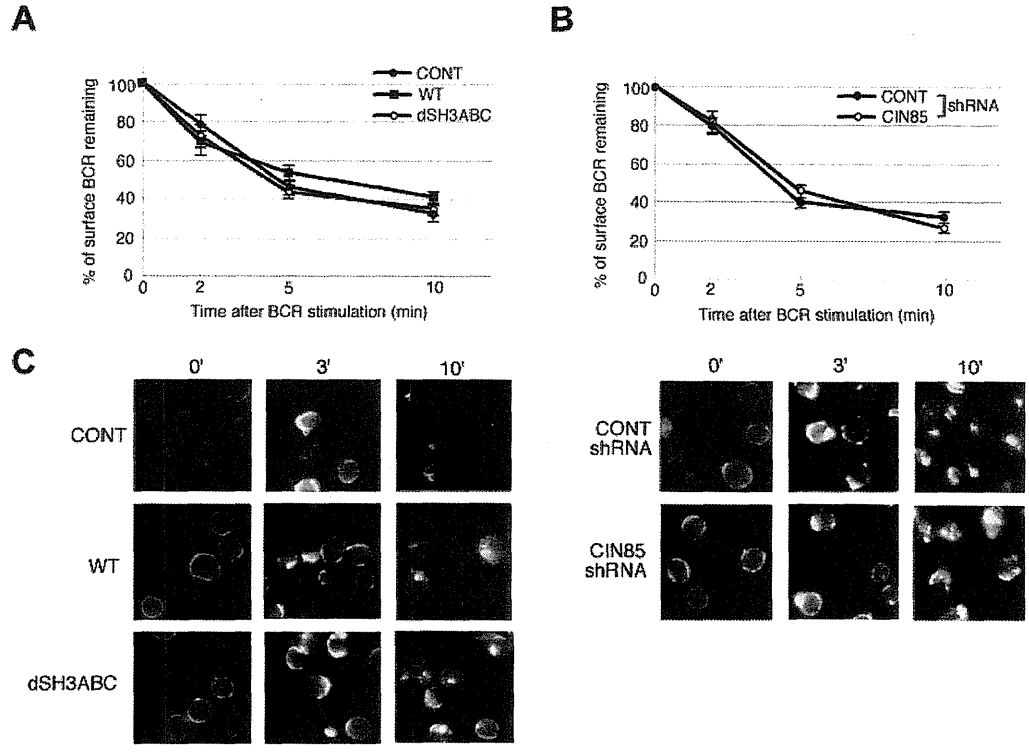

Figure 5. CIN85 does not affect BCR internalization. (A) BJAB cells (control and stable transformants expressing either WT or SH3-deleted CIN85) and (B) BJAB cells (control and CIN85-knockdown) were incubated at 4°C with $F(ab')_2$ goat anti–human IgM for 30 minutes. The cells were washed, warmed to 37°C for the indicated time intervals, stained at 4°C for 30 minutes with a FITC-labeled anti–goat IgG pAb, and analyzed by flow cytometry. The results are expressed as the percentage of surface BCRs remaining. The data are presented as the average and SEM of 3 independent experiments. (C) Control BJAB cells, stable transformants expressing either WT or SH3-deleted CIN85, and CIN85-knockdown BJAB cells were incubated at 4°C with 20 μg/mL $F(ab')_2$ goat anti–human IgM for 30 minutes. The cells were washed and warmed to 37°C for the indicated time periods. The cells were fixed, permeabilized, stained with a FITC-labeled anti–goat IgG pAb, and analyzed by fluorescence microscopy. The images shown are representative of 3 independent experiments.

function of coated vesicles.[25] Similarly, early studies showed a characteristic feature of CIN85 in the formation of clathrin-coated vesicles during the internalization of RTKs such as EGFRs in nonimmune cells.[18,19] Brain-specific CIN85-deficient mice manifest impaired internalization of D2 dopamine receptors, which belong to the 7-transmembrane G protein-coupled receptor superfamily.[38] In addition, CIN85 facilitates ligand-induced FcεRI internalization in RBL-2H3 mast cell lines.[20] Because BCR internalization is regulated via a clathrin-dependent pathway,[39] it was of interest to determine whether CIN85 regulates BCR internalization. Our study, however, shows that CIN85 does not affect BCR internalization (Figure 5, supplemental Figure 1). These data are somewhat surprising, given that Cbl proteins control BCR internalization by a ubiquitin-dependent mechanism.[10,40] However, the role of Cbl proteins in BCR ubiquitination and internalization is still rather controversial. The HECT family member Itch, but not c-Cbl, is an E3 ubiquitin ligase that is involved in BCR ubiquitination.[41] In addition, the ubiquitination of Igβ, which is a component of BCR, does not facilitate BCR internalization but is required for the sorting of early endosomes and for trafficking into late endosomes,[41] which suggests that BCR ubiquitination is more critical at the later stage of its trafficking. Because our imaging analysis (Figure 5C) cannot clearly distinguish the spatial distribution of early and late endosomes, it is of great interest to test whether CIN85 affects postendocytotic BCR trafficking. A recent study showed that in human neutrophils, CIN85 modulates c-Cbl–mediated down-regulation of FcγRIIa in the later stages of receptor trafficking without affecting the internalization of this receptor.[22]

During the submission of this paper, 2 studies were published that, in contrast to our findings, showed that CIN85 positively regulates BCR signaling in mouse and chicken B cells.[42,43] These studies found that CIN85 associates with BLNK and regulates BCR-induced NF-κB activation. However, the detailed profiles of BCR signaling differ between the 2 studies: the BCR-induced phosphorylation of BLNK and PLCγ2 and the calcium flux are significantly decreased on the loss of CIN85 in chicken B cells, whereas they are apparently normal in CIN85-deficient mouse B cells.[42,43] It should be noted that the former study did not actually use CIN85-deficient cells; rather, it used cells expressing a mutant BLNK that failed to bind to CIN85 or its homolog CD2AP.[42] Although these findings are intriguing, it is rather surprising that Cbl-mediated function of CIN85 in B cells was barely investigated in these studies. As previously mentioned, it is becoming evident that Cbl proteins play a critical role in the function of CIN85 in immune cells.[20-22] In addition, BCR-induced association of CIN85 with c-Cbl was recently shown even in mouse B cells.[44] We thus find that in human B cells, CIN85 negatively regulates BCR signaling via a Cbl-dependent mechanism. Our data obtained using CIN85-knockdown primary B cells also support this hypothesis. The molecular reason underlying the apparent discrepancy between our study and the aforementioned ones[42,43] remains unclear. One possibility, however, is that the relative contribution of CIN85-binding partners varies depending on the source of B cells used. In human B cells, Cbl proteins seem to preferentially associate with CIN85 over BLNK (Figure 1A). Notably, we found that CD2AP seems to preferentially associate with BLNK over c-Cbl in human B cells (supplemental Figure 2). It is therefore of potential interest

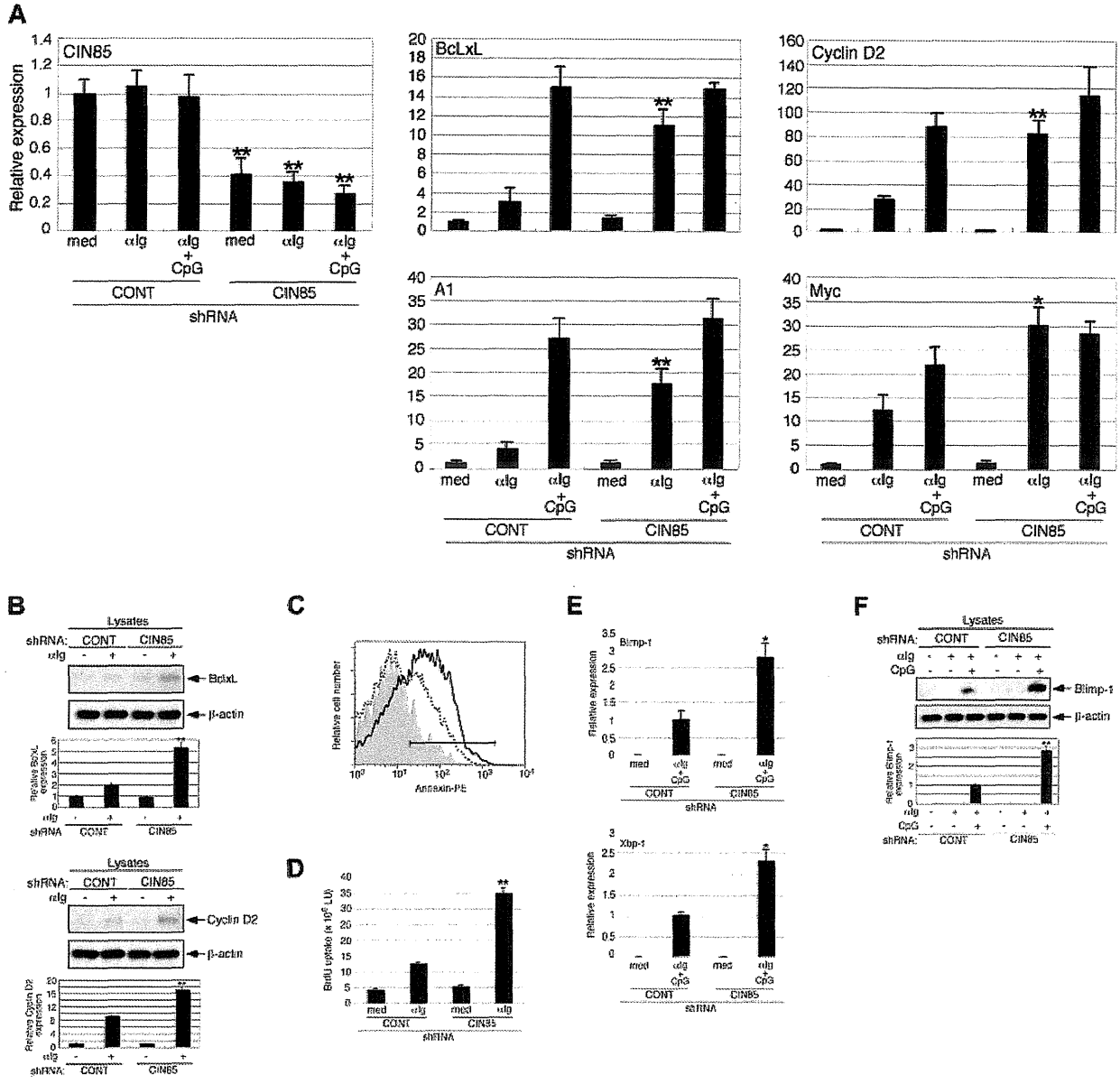

Figure 6. CIN85 knockdown enhances the survival, growth, and differentiation of primary B cells. (A) Control and CIN85-knockdown primary B cells were incubated for 24 hours in medium containing F(ab')$_2$ goat anti–human IgG/IgA/IgM (αIg, 20 μg/mL) or αIg plus CpG (1 μM), and CIN85, BcLxL, A1, cyclin D2, and myc mRNA levels were quantified by real-time PCR. The data are normalized to the expression of 18S rRNA. The results shown are representative of 3 independent experiments (*$P < .05$, **$P < .01$ vs controls). (B) Control and CIN85-knockdown primary B cells were incubated for 24 hours in the absence or presence of F(ab')$_2$ goat anti–human IgG/IgA/IgM (αIg, 20 μg/mL). The cell lysates were subsequently separated on a SDS-PAGE gel and analyzed by Western blotting with anti-BclxL mAb, anti-cyclin D2 pAb, or anti–β-actin mAb. The resulting values are expressed as fold changes in protein expression compared with nonstimulated control cells. The values are the mean ± SD of 3 independent experiments (**$P < .01$ vs controls). (C) Control and CIN85-knockdown primary B cells were incubated for 48 hours in the absence or presence of F(ab')$_2$ goat anti–human IgG/IgA/IgM (αIg, 20 μg/mL). After culture, the cells were stained with PE-labeled annexin V and analyzed using flow cytometry. The percentages of annexin-positive cells are shown. A representative histogram of 3 independent experiments is shown. (D) Control and CIN85-knockdown primary B cells were incubated for 48 hours in the absence or presence of F(ab')$_2$ goat anti–human IgG/IgA/IgM (αIg, 20 μg/mL). After culture, the cells were pulsed with BrdU, and its incorporation was detected by incubation with anti-BrdU mAb, followed by rhodamine-conjugated anti–mouse Ab. A representative histogram of 3 independent experiments is shown (**$P < .01$ vs controls). (E) Control and CIN85-knockdown primary B cells were incubated for 48 hours in the absence or presence of F(ab')$_2$ goat anti–human IgG/IgA/IgM (αIg, 20 μg/mL) and CpG (1 μM), and quantitation of Blimp-1 and Xbp-1 mRNA by real-time PCR was carried out. The data are normalized to the expression of 18S rRNA. The results shown are representative of 3 independent experiments (*$P < .05$ vs controls). (F) Control and CIN85-knockdown primary B cells were incubated for 48 hours with or without F(ab')$_2$ goat anti–human IgG/IgA/IgM (αIg, 20 μg/mL) in the absence or presence of CpG (1 μM). The cell lysates were subsequently separated on a SDS-PAGE gel and analyzed by Western blotting with anti–Blimp-1 mAb or anti–β-actin mAb. The resulting values are expressed as fold changes in protein expression compared with unstimulated control cells. The values are the mean ± SD of 3 independent experiments (**$P < .01$ vs controls).

to compare the roles of CIN85 and CD2AP in the function of human B cells.

BCR signals play a pivotal role in the survival, growth, and differentiation of B cells.[1,2] Under physiologic conditions, BCR signaling is fine-tuned by positive and negative regulators and is generally insufficient for the full activation of B cells, rendering them susceptible to apoptosis and anergy. However, when the negative regulation of BCR signaling is compromised, unwanted B cells could grow and survive, thereby potentially leading to autoimmunity and B-cell malignancies. This study showed that

CIN85 knockdown in primary B cells causes full activation of B cells and enhances BCR-induced survival and growth via the increased expression of BcLxL, A1, cyclin D2, and myc (Figure 6). Given that Cbl proteins are critical for B-cell anergy,[10] CIN85 may cooperate with Cbl proteins to function as a key negative regulator for BCR signaling and to maintain self-tolerance. It is thus of interest to determine whether the expression and/or function of CIN85 could be altered in human autoimmune diseases such as SLE. Surprisingly, CLL cells from advanced-stage patients exhibit hypophosphorylation of c-Cbl,[11] as seen in CIN85-knockdown cells. The manipulation of CIN85 expression may therefore provide a novel strategy to control aberrant cell growth and survival in B-cell malignancies.

Acknowledgments

The authors thank Editage for proofreading the English used in this paper.

This work was supported in part by a Grant-in-Aid from the Ministry of Education, Culture, Sports, Science, and Technology of Japan (H.N. and K.A.).

Authorship

Contribution: H.N. and K.A. designed and performed the research, analyzed the data, and wrote the paper; S.J.-T., Y.K., T.S., K.N., S.-i.O., H. Tsuzuki, Y.I., Y.A., H.I., S.S., E.B., H. Tsukamoto, and T.H. performed the research; and T.T. provided cDNA constructs and helped write the paper.

Conflict-of-interest disclosure: The authors declare no competing financial interests.

Correspondence: Hiroaki Niiro, Dept of Medicine and Biosystemic Science, Graduate School of Medical Sciences, Kyushu University, 3-1-1 Maidashi, Higashi-ku, Fukuoka 812-8582, Japan; e-mail: hniiro@med.kyushu-u.ac.jp.

References

1. Niiro H, Clark EA. Regulation of B-cell fate by antigen-receptor signals. *Nat Rev Immunol.* 2002;2(12):945-956.
2. Kurosaki T, Shinohara H, Baba Y. B cell signaling and fate decision. *Annu Rev Immunol.* 2010;28: 21-55.
3. Pogue SL, Kurosaki T, Bolen J, Herbst R. B cell antigen receptor-induced activation of Akt promotes B cell survival and is dependent on Syk kinase. *J Immunol.* 2000;165(3):1300-1306.
4. Thien CB, Langdon WY. c-Cbl and Cbl-b ubiquitin ligases: substrate diversity and the negative regulation of signalling responses. *Biochem J.* 2005; 391(pt 2):153-166.
5. Liu YC, Gu H. Cbl and Cbl-b in T-cell regulation. *Trends Immunol.* 2002;23(3):140-143.
6. Swaminathan G, Tsygankov AY. The Cbl family proteins: ring leaders in regulation of cell signaling. *J Cell Physiol.* 2006;209(1):21-43.
7. Duan L, Reddi AL, Ghosh A, Dimri M, Band H. The Cbl family and other ubiquitin ligases: destructive forces in control of antigen receptor signaling. *Immunity.* 2004;21(1):7-17.
8. Panchamoorthy G, Fukazawa T, Miyake S, et al. p120cbl is a major substrate of tyrosine phosphorylation upon B cell antigen receptor stimulation and interacts in vivo with Fyn and Syk tyrosine kinases, Grb2 and Shc adaptors, and the p85 subunit of phosphatidylinositol 3-kinase. *J Biol Chem.* 1996;271(6):3187-3194.
9. Yasuda T, Maeda A, Kurosaki M, et al. Cbl suppresses B cell receptor-mediated phospholipase C (PLC)-gamma2 activation by regulating B cell linker protein-PLC-gamma2 binding. *J Exp Med.* 2000;191(4):641-650.
10. Kitaura Y, Jang IK, Wang Y, et al. Control of the B cell-intrinsic tolerance programs by ubiquitin ligases Cbl and Cbl-b. *Immunity.* 2007;26(5):567-578.
11. Mankai A, Eveillard JR, Buhe V, et al. Is the c-Cbl proto-oncogene involved in chronic lymphocytic leukemia? *Ann N Y Acad Sci.* 2007;1107:193-205.
12. Niiro H, Maeda A, Kurosaki T, Clark EA. The B lymphocyte adaptor molecule of 32 kD (Bam32) regulates B cell antigen receptor signaling and cell survival. *J Exp Med.* 2002;195(1): 143-149.
13. Niiro H, Allam A, Stoddart A, Brodsky FM, Marshall AJ, Clark EA. The B lymphocyte adaptor molecule of 32 kilodaltons (Bam32) regulates B cell antigen receptor internalization. *J Immunol.* 2004;173(9):5601-5609.
14. Take H, Watanabe S, Takeda K, Yu ZX, Iwata N, Kajigaya S. Cloning and characterization of a novel adaptor protein, CIN85, that interacts with c-Cbl. *Biochem Biophys Res Commun.* 2000; 268(2):321-328.
15. Gout I, Middleton G, Adu J, et al. Negative regulation of PI 3-kinase by Ruk, a novel adaptor protein. *EMBO J.* 2000;19(15):4015-4025.
16. Bogler O, Furnari FB, Kindler-Roehrborn A, et al. SETA: a novel SH3 domain-containing adapter molecule associated with malignancy in astrocytes. *Neuro Oncol.* 2000;2(1):6-15.
17. Narita T, Amano F, Yoshizaki K, et al. Assignment of SH3KBP1 to human chromosome band Xp22.1–>p21.3 by in situ hybridization. *Cytogenet Cell Genet.* 2001;93(1-2):133-134.
18. Petrelli A, Gilestro GF, Lanzardo S, Comoglio PM, Migone N, Giordano S. The endophilin-CIN85-Cbl complex mediates ligand-dependent downregulation of c-Met. *Nature.* 2002;416(6877):187-190.
19. Soubeyran P, Kowanetz K, Szymkiewicz I, Langdon WY, Dikic I. Cbl-CIN85-endophilin complex mediates ligand-induced downregulation of EGF receptors. *Nature.* 2002;416(6877):183-187.
20. Molfetta R, Belleudi F, Peruzzi G, et al. CIN85 regulates the ligand-dependent endocytosis of the IgE receptor: a new molecular mechanism to dampen mast cell function. *J Immunol.* 2005; 175(7):4208-4216.
21. Peruzzi G, Molfetta R, Gasparrini F, et al. The adaptor molecule CIN85 regulates Syk tyrosine kinase level by activating the ubiquitin-proteasome degradation pathway. *J Immunol.* 2007;179(4):2089-2096.
22. Marois L, Vaillancourt M, Pare G, et al. CIN85 modulates the down-regulation of Fc gammaRIIa expression and function by c-Cbl in a PKC-dependent manner in human neutrophils. *J Biol Chem.* 2011;286(17):15073-15084.
23. Tabrizi SJ, Niiro H, Masui M, et al. T cell leukemia/lymphoma 1 and galectin-1 regulate survival/cell death pathways in human naive and IgM+ memory B cells through altering balances in Bcl-2 family proteins. *J Immunol.* 2009;182(3):1490-1499.
24. Narita T, Nishimura T, Yoshizaki K, Taniyama T. CIN85 associates with TNF receptor 1 via Src and modulates TNF-alpha-induced apoptosis. *Exp Cell Res.* 2005;304(1):256-264.
25. Havrylov S, Rzhepetskyy Y, Malinowska A, Drobot L, Redowicz MJ. Proteins recruited by SH3 domains of Ruk/CIN85 adaptor identified by LC-MS/MS. *Proteome Sci.* 2009;7:21.
26. Watanabe S, Take H, Takeda K, Yu ZX, Iwata N, Kajigaya S. Characterization of the CIN85 adaptor protein and identification of components involved in CIN85 complexes. *Biochem Biophys Res Commun.* 2000;278(1):167-174.
27. Chiu CW, Dalton M, Ishiai M, Kurosaki T, Chan AC. BLNK: molecular scaffolding through 'cis'-mediated organization of signaling proteins. *EMBO J.* 2002;21(23):6461-6472.
28. Marshall AJ, Niiro H, Yun TJ, Clark EA. Regulation of B-cell activation and differentiation by the phosphatidylinositol 3-kinase and phospholipase Cgamma pathway. *Immunol Rev.* 2000;176:30-46.
29. Turner M. B-cell development and antigen receptor signalling. *Biochem Soc Trans.* 2002;30(4): 812-815.
30. Peng SL, Gerth AJ, Ranger AM, Glimcher LH. NFATc1 and NFATc2 together control both T and B cell activation and differentiation. *Immunity.* 2001;14(1):13-20.
31. Rao N, Ghosh AK, Ota S, et al. The non-receptor tyrosine kinase Syk is a target of Cbl-mediated ubiquitylation upon B-cell receptor stimulation. *EMBO J.* 2001;20(24):7085-7095.
32. Sohn HW, Gu H, Pierce SK. Cbl-b negatively regulates B cell antigen receptor signaling in mature B cells through ubiquitination of the tyrosine kinase Syk. *J Exp Med.* 2003;197(11):1511-1524.
33. Su TT, Rawlings DJ. Transitional B lymphocyte subsets operate as distinct checkpoints in murine splenic B cell development. *J Immunol.* 2002; 168(5):2101-2110.
34. Yi AK, Chang M, Peckham DW, Krieg AM, Ashman RF. CpG oligodeoxyribonucleotides rescue mature spleen B cells from spontaneous apoptosis and promote cell cycle entry. *J Immunol.* 1998;160(12):5898-5906.
35. Calame KL, Lin KI, Tunyaplin C. Regulatory mechanisms that determine the development and function of plasma cells. *Annu Rev Immunol.* 2003;21:205-230.
36. Turner M, Schweighoffer E, Colucci F, Di Santo JP, Tybulewicz VL. Tyrosine kinase SYK: essential functions for immunoreceptor signalling. *Immunol Today.* 2000;21(3):148-154.

37. Stamenova SD, French ME, He Y, Francis SA, Kramer ZB, Hicke L. Ubiquitin binds to and regulates a subset of SH3 domains. *Mol Cell.* 2007; 25(2):273-284.

38. Shimokawa N, Haglund K, Holter SM, et al. CIN85 regulates dopamine receptor endocytosis and governs behaviour in mice. *EMBO J.* 2010; 29(14):2421-2432.

39. Stoddart A, Dykstra ML, Brown BK, Song W, Pierce SK, Brodsky FM. Lipid rafts unite signaling cascades with clathrin to regulate BCR internalization. *Immunity.* 2002;17(4):451-462.

40. Jacob M, Todd L, Sampson MF, Pure E. Dual role of Cbl links critical events in BCR endocytosis. *Int Immunol.* 2008;20(4):485-497.

41. Zhang M, Veselits M, O'Neill S, et al. Ubiquitinylation of Ig beta dictates the endocytic fate of the B cell antigen receptor. *J Immunol.* 2007;179(7): 4435-4443.

42. Oellerich T, Bremes V, Neumann K, et al. The B-cell antigen receptor signals through a preformed transducer module of SLP65 and CIN85. *EMBO J.* 2011;30(17):3620-3634.

43. Kometani K, Yamada T, Sasaki Y, et al. CIN85 drives B cell responses by linking BCR signals to the canonical NF-kappaB pathway. *J Exp Med.* 2011;208(7):1447-1457.

44. Buchse T, Horras N, Lenfert E, et al. CIN85 interacting proteins in B cells-specific role for SHIP-1. *Mol Cell Proteomics.* 2011;10(10):M110.

Engulfment of hematopoietic stem cells caused by down-regulation of CD47 is critical in the pathogenesis of hemophagocytic lymphohistiocytosis

Takuro Kuriyama,[1] Katsuto Takenaka,[1] Kentaro Kohno,[2] Takuji Yamauchi,[1] Shinya Daitoku,[1] Goichi Yoshimoto,[3] Yoshikane Kikushige,[1] Junji Kishimoto,[4] Yasunobu Abe,[5] Naoki Harada,[3] Toshihiro Miyamoto,[1] Hiromi Iwasaki,[2] Takanori Teshima,[2] and Koichi Akashi[1,2]

[1]Department of Medicine and Biosystemic Science, Kyushu University Graduate School of Medical Sciences, Fukuoka, Japan; [2]Center for Cellular and Molecular Medicine, Kyushu University Hospital, Fukuoka, Japan; [3]Department of Hematology, Kyushu Medical Center, Fukuoka, Japan; [4]Digital Medicine Initiative, Kyushu University, Fukuoka, Japan; and [5]Department of Medicine and Bioregulatory Science, Kyushu University Graduate School of Medical Sciences, Fukuoka, Japan

Hemophagocytic lymphohistiocytosis (HLH) is characterized by deregulated engulfment of hematopoietic stem cells (HSCs) by BM macrophages, which are activated presumably by systemic inflammatory hypercytokinemia. In the present study, we show that the pathogenesis of HLH involves impairment of the antiphagocytic system operated by an interaction between surface CD47 and signal regulatory protein α (SIRPA). In HLH patients, changes in expression levels and HLH-specific polymorphism of SIRPA were not found. In contrast, the expression of surface CD47 was down-regulated specifically in HSCs in association with exacerbation of HLH, but not in healthy subjects. The number of BM HSCs in HLH patients was reduced to approximately 20% of that of healthy controls and macrophages from normal donors aggressively engulfed HSCs purified from HLH patients, but not those from healthy controls in vitro. Furthermore, in response to inflammatory cytokines, normal HSCs, but not progenitors or mature blood cells, down-regulated CD47 sufficiently to be engulfed by macrophages. The expression of prophagocytic calreticulin was kept suppressed at the HSC stage in both HLH patients and healthy controls, even in the presence of inflammatory cytokines. These data suggest that the CD47-SIRPA antiphagocytic system plays a key role in the maintenance of HSCs and that its disruption by HSC-specific CD47 down-regulation might be critical for HLH development. (*Blood.* 2012;120(19):4058-4067)

Introduction

Hemophagocytic lymphohistiocytosis (HLH) is a syndrome with excessive immune activation characterized by deregulated engulfment of hematopoietic cells by macrophages in the BM. Patients with HLH display hemophagocytosis, pancytopenia, and various inflammatory symptoms, including high fever, acute liver failure, and splenomegaly.[1-4] HLH is classified into primary HLH and secondary HLH. Primary HLH, also known as familial hemophagocytic lymphohistiocytosis, shows clear familial inheritance or genetic causes, including mutations in the perforin (PRF1), MUNC13-4, syntaxin 11 (STX11), and RAB27A genes.[5-9] In primary HLH, natural killer cells and/or cytotoxic T lymphocytes fail to eliminate the targets in response to inflammatory reactions, and the resulting sustained inflammatory responses induce deregulated activation of macrophages. In secondary HLH, macrophages are activated in association with infections and malignant disorders.[4] The key pathogenic feature of HLH is hypercytokinemia including IFN-γ, TNF-α, IL-6, and M-CSF, which may activate macrophages to engulf blood cells.[3] These cytokines are produced mainly by natural killer cells and cytotoxic T lymphocytes, and might stimulate BM macrophages to engulf erythrocytes, leukocytes, platelets, and their precursors in the BM.

The question is, if hypercytokinemia causes activation of macrophages to engulf blood cells, why does such activation occur specifically in BM macrophages and induce severe hypocellularity and pancytopenia? Engulfment is triggered by the binding of specific receptors on macrophages to their ligands. Receptors on macrophages include phosphatidylserine receptors and low-density lipoprotein-related protein (LRP).[10-14] Lipopolysaccharide and calreticulin (CRT) are typical ligands for these macrophage receptors to induce a prophagocytic signal.[14,15] The phosphatidylserine-phosphatidylserine receptor system predominantly serves as a prophagocytic signal for macrophages during apoptosis.[13,16] In contrast, the CRT-LRP system also works on viable cells,[14] so there must be a mechanism to prevent inadequate engulfment of viable cells. Self-recognition to prevent phagocytosis is regulated by the CD47 and signal regulatory protein α (SIRPA) interaction, and CD47-SIRPA signaling plays an important role in preventing phagocytosis of cells.[17,18] Therefore, phagocytosis of viable cells is regulated by the balance of prophagocytic CRT-LRP and antiphagocytic CD47-SIRPA signals for macrophages, indicating that the balance of this signaling is deregulated in HLH.

CD47 is a member of the Ig superfamily that is ubiquitously expressed in hematopoietic and nonhematopoietic cells.[17,18] CD47 interacts with SIRPA through its respective IgV-like domains.[18] In contrast, SIRPA is a transmembrane protein that contains 3 Ig-like domains within the extracellular region. SIRPA is expressed in macrophages, myeloid cells, and neurons.[18-21] The cytoplasmic region of SIRPA has immunoreceptor tyrosine-based inhibitory

Submitted February 5, 2012; accepted August 26, 2012. Prepublished online as *Blood* First Edition paper, September 18, 2012; DOI 10.1182/blood-2012-02-408864.

The online version of this article contains a data supplement.

The publication costs of this article were defrayed in part by page charge payment. Therefore, and solely to indicate this fact, this article is hereby marked "advertisement" in accordance with 18 USC section 1734.

motifs.[18] Binding cell-surface CD47 with SIRPA on macrophages provokes inhibitory signals through phosphorylation of the immunoreceptor tyrosine-based inhibitory motifs of SIRPA, activating inhibitory tyrosine phosphatases such as SHP1 and SHP2.[18] This signaling inhibits myosin assembly of macrophages, thereby inhibiting phagocytosis.[18] The CD47-SIRPA self-recognition system is primarily used in RBC clearance to maintain homeostasis of the blood.[22]

Interestingly, this system also plays a critical role in engraftment of hematopoietic stem cells (HSCs) in xenotransplantation. Transplantation of the BM of CD47-deficient mice could not rescue lethally irradiated wild-type mice,[23] probably due to engulfment of CD47-deficient HSCs by BM macrophages that constitute the HSC niche.[24,25] In addition, we have reported previously that polymorphism of the SIRPA IgV domain can modulate the binding affinity of mouse SIRPA to human CD47 and plays a decisive role in xenotransplantation of human HSCs into mice; NOD, a mouse line known to have very efficient engraftment of human hematopoiesis, has a SIRPA polymorphism that can recognize human CD47, and this binding produces inhibitory signaling for mouse macrophages not to engulf human HSCs.[26]

These previous data led us to hypothesize that the BM-specific macrophage activation in HLH is caused by disruption of the CD47-SIRPA self-recognition system. In the present study, we show that in HLH, inflammatory cytokines down-regulate CD47, especially at the HSC stage, which can provoke the engulfment of HSCs by macrophages.

Methods

Patients and samples

Supplemental Table 1 (available on the *Blood* Web site; see the Supplemental Materials link at the top of the online article) summarizes the clinical characteristics of the patients. During the period from October 2005 to April 2011, 24 patients were diagnosed with HLH. The diagnosis of HLH was made according to HLH-2004 diagnostic guideline[27] and Tsuda-97.[28] The median age was 36 years (range, 16-71). Etiologies were documented in 12 patients: EBV (n = 7), CMV (n = 1), diffuse large B-cell lymphoma (n = 1), EBV^+ diffuse large B-cell lymphoma (n = 1), defective PRF1 (n = 1), and adult onset Still disease (n = 1). The median hemoglobin level was 11.1 g/dL (range, 6.2-16.2), the median platelet count was 54.8×10^9/L (range, 4-187), and the median ferritin level was 4530 ng/mL (range, 620-44 020). Prednisolone-based treatment was used in 14 patients (58%), and HSC transplantation was performed in 2 patients (8%). BM and peripheral blood samples were obtained from healthy volunteers (n = 50) and HLH patients (n = 24). Cord blood samples from full-term deliveries and normal BM samples from normal volunteers were obtained based on informed consent (provided by Kyushu Block Red Cross Blood Center, Japan Red Cross Society). Informed consent was received for all donors in accordance with the Declaration of Helsinki. The institutional review board of Kyushu University Hospital approved all experiments in this study.

Cell lines

A human acute promyelocytic leukemia cell line, NB4, which retains t(15;17), was obtained from the German Collection of Microorganisms and Cell Cultures (DSMZ). NB4 cells were cultured in RPMI 1640 medium (Wako) containing 10% FBS (ICN).

Sequence alignment of the human SIRPA IgV domains

Genomic DNA was extracted by using QIAamp DNA Blood Mini Kit (QIAGEN). The cording region of the SIRPA IgV domain was amplified by PCR. Genomic DNA was used as a PCR template in the following conditions: 10 minutes at 94°C, 30 cycles of 1 minute at 94°C, 1 minute at 60°C, 1 minute at 72°C, and 16 minutes at 72°C. PCR and sequencing primers were as follows: forward primer 5′-GCCTGCTTC-TGGTGTGCATCCAGTC-3′ reverse primer 5′-GAGTTACTGTC-ACAAACCAGAGGC-3′. PCR products were cloned to the PCR 2.1-TOPO vector (Invitrogen) and 10-25 clones were sequenced for every sample.

Abs, cell staining, and sorting

For analysis of cell-surface expression of SIRPA, we used SIRPA mAb (MBL International) and FITC-conjugated antimouse IgG (Beckman Coulter). For analysis of cell-surface expression of CD47, we used PE-conjugated anti-CD47 (BD Pharmingen). For sorting and analysis of $CD34^+CD38^-$ and $CD34^+CD38^+$ cells, cells were stained with FITC-conjugated anti-CD34 (BD Pharmingen), PE-conjugated anti-CRT (Enzo Life Sciences), peridinin chlorophyll A protein-cy5.5–conjugated anti-CD47 (BD Pharmingen), and allophycocyanin-conjugated anti-CD38 (BD Pharmingen). For some experiments, cells were stained with allophycocyanin-conjugated anti-CD34, PE-conjugated anti-CD47, and PE-Cy7 conjugated anti-CD38 (all BD Pharmingen). Before sorting and analysis, lineage cells in cord blood cells were depleted using a lineage cell depletion kit (Miltenyi Biotec). $CD34^+CD38^-$ and $CD34^+CD38^+$ cells were purified on a FACSAria cell sorter (BD Biosciences).

The analysis procedures of $CD34^+CD38^+$ progenitor populations were described previously.[29,30] BM mononuclear cells were first stained with PE-Cy5–conjugated lineage Abs, including anti-CD3, anti-CD4, anti-CD8, anti-CD10, anti-CD19, anti-CD20, anti-CD14, anti-CD56, and glycophorin A (BD Pharmingen). Subsequently, cells were stained with FITC-conjugated anti-CD34 (BD Pharmingen), PE-conjugated anti-CD47 (BD Pharmingen), PE-Cy7–conjugated anti-CD123 (eBiosciences), and Pacific Blue–conjugated anti-CD45RA (Beckman Coulter) Abs. HSCs, common myeloid progenitors, granulocyte/macrophage progenitors, and megakaryocyte/erythrocyte progenitors were isolated as $Lin^-CD34^+CD38^-$, $Lin^-CD34^+CD38^+CD123^+CD45RA^-$, $Lin^-CD34^+CD38^+CD123^+CD45RA^+$, and $Lin^-CD34^+CD38^+CD123^-CD45RA^-$ populations. The cells were analyzed and sorted with a FACSCalibur flow cytometer and a FACSAria 2 cell sorter (both BD Biosciences). The mean fluorescent intensity of CD47 and CRT was normalized and shown as a ratio to PBMCs from healthy donors.

Preparation of human macrophages from peripheral blood

Monocytes were purified from PBMCs by positive selection using MACS CD14 Micro Beads (Miltenyi Biotec). These cells were incubated with X-VIVO10 (Lonza) containing 2% AB serum and 100 ng/mL of M-CSF (R&D Systems) for more than 96 hours to obtain macrophages.[31,32]

In vitro phagocytosis assays for target cells

Peripheral blood–derived macrophages were prepared and incubated at 1.0×10^4 cells in 200 μL of RPMI 1640 medium in Falcon culture tubes (2058; BD Biosciences), and then $1.0\text{-}5.0 \times 10^4$ target cells were added to the tubes and incubated at 37°C for 2 hours. Before the addition of target cells to macrophage-containing tubes, cells were opsonized with CD34 Ab (sc-19621; Santa Cruz Biotechnology) for $CD34^+CD38^-$ cells and $CD34^+CD38^+$ cells isolated from normal and HLH BM by FACS sorting; CD13 Ab (sc-51522; Santa Cruz Biotechnolgoy) and CD33 Ab (sc-19660; Santa Cruz Biotechnology) for NB4 cells; CD45 Ab (555480; BD Pharmingen) for lymphocytes; and neutrophils and glycophorin A Ab for RBCs (555569; BD Pharmingen). For activation of macrophages, cells were incubated with IFN-γ (100 ng/mL; R&D Systems) for 24 hours and with lipopolysaccharide (0.3 μg/μL) for 1 hour, and then harvested and washed 3 times with PBS before the addition of target cells. After coincubation with macrophages and target cells, they were mounted on cytospin preparations, and 1000 macrophages were tested to enumerate engulfing ones by a blinded observer. We calculated the phagocytic index using the following formula: phagocytosis index = phagocytic macrophages/number of macrophages.[33]